ELSEVIER

Polymer 42 (2001) 2137–2165

polymer

www.elsevier.nl/locate/polymer

Recycling of natural rubber latex waste and its interaction in epoxidised natural rubber

G. Mathew[a], R.P. Singh[b], N.R. Nair[c], S. Thomas[d,*]

[a]*Department of Chemistry, C.M.S. College, Kottayam 686001, Kerala, India*
[b]*Polymer Chemistry Division, National Chemical Lab, Pune 411008, India*
[c]*Rubber Research Institute of India, Kottayam 686009, Kerala, India*
[d]*School of Chemical Sciences, Mahatma Gandhi University, Kottayam 686560, Kerala, India*

Received 27 October 1998; received in revised form 5 April 2000; accepted 13 June 2000

Abstract

The waste rubber formed in latex-based industries is around 10–15% of the rubber consumed. The formation of a higher percentage of waste latex rubber (WLR) in latex factories is due to the unstable nature of the latex compound and the strict specifications in the quality of latex products. These latex rejects contain about 95% rubber hydrocarbon of very high quality, which is only lightly cross-linked. These rejects, if not properly used, can create serious ecological and environmental problems. The authors have developed a cost-effective technique for the reuse of WLR in epoxidised natural rubber (ENR). The effect of powdered rejects on the curing behaviour, mechanical performance and swelling nature has been investigated. The cure characteristics such as optimum cure time, rheometric scorch time and induction time, are found to decrease with increasing concentration of latex waste filler. When the vulcanisation system is conventional, the finest size filler shows superior mechanical performance while the order of performance is reversed when the vulcanisation mode changes to efficient. The applications and limitations of several theoretical models in describing the tensile modulus of the samples have been demonstrated. A three-layer model has been used to study the migration of sulphur from ENR to the latex filler phase. The extent of sulphur migration in the case of different particle sizes of latex waste filler in two different vulcanisation systems has been analysed. The failure behaviour of the samples was analysed using scanning electron microscopy. The study shows that waste latex rubber can be used as filler in ENR economically.

Keywords: Rubber recycling; Epoxidised natural rubber; Processing characteristics

1. Introduction

Elastomers are a major class of materials having a wide range of applications, ranging from footwear to space vehicles. This is because of their unique mechanical properties such as elastic behaviour even at very large deformation and energy absorbing capacity. By properly controlling the compounding ingredients in rubber, its ultimate properties can be made to match the requirements. The potential properties of an elastomer can be improved by the addition of certain fillers like silica, carbon black, mica [1,2], etc. As a result of the severe energy crisis, and the need to reduce compound cost, rubber product manufacturers were forced to increase the proportion of filler in the rubber compound without adversely affecting the mechanical properties. This approach, however, always resulted in a rubber compound with very high specific gravity [3], which is not fair, as far as elastomers are concerned. In order to overcome this problem and also to make the rubber compound cheaper, new materials have been considered for use as fillers. Just like waste plastic, waste rubber also is becoming a world-wide problem. The disposal/utilisation of tyres, whose life span has ended, is a great economic and ecological problem. The earlier approach to this problem was to reclaim [4] or remove the cross-links in the rubber rejects and then use the latter as new rubber. However, the use of reclaimed rubber was limited owing to three main reasons:

(i) Easy reclamation was not possible in the case of waste tyres due to the presence of steel belts or plies [5].
(ii) The properties of reclaimed rubber were inferior due to its degradation during reclamation.
(iii) The various components of a tyre or blend may not respond in the same way to reclamation [6].

Meanwhile the authorities prohibit the open burning of this waste because of the release of zinc compounds into the

* Corresponding author. Tel.: +91-481-598303; fax: +91-481-561190.
E-mail address: sabut@md4.vsnl.net.in (S. Thomas).

0032-3861/01/$ - see front matter
PII: S0032-3861(00)00492-4

atmosphere [7]. Therefore, nowadays researchers pay more attention to scrap latex rejects compared to reclaimed rubber. This is because of the lightly cross-linked and high-quality nature of the rubber obtainable from latex rejects. Moreover, these rejects are available in huge quantities. The two main reasons for this surplus nature are the unstable nature of latex and the strict specifications regarding the quality of latex products. Therefore, these scrap latex rejects are now considered as the best potential candidate for recycling.

Many reviews regarding the disposal problem of rubber rejects and possible solutions are available from the literature [8–11]. Another method to reuse large volumes of scrap latex rejects to use it as an impact modifier in brittle plastics like polystyrene [5,12]. This can be done simply, either by solution or melt blending techniques, or by polymerising the monomer in the presence of swollen crumb, as done by Freeguard [13]. Researchers [14] have analysed the reactive blending of plastics and scrap rubber also. The use of cryoground rejects, as filler in rubbers [8,9] and polyolefins [15] is well known. Recently, many new methods for the devulcanisation of waste rubber have become available. The most important among these is the devulcanisation process using ultrasonic irradiation. A number of studies in this field have been reported by Tukachinsky [16], Levin [17] and Isayev et al. [18,19]. They found that in the presence of heat and temperature, the ultrasonic waves were able to break up the three-dimensional network in cross-linked rubbers. The resulting devulcanised rubber could be reprocessed, shaped and revulcanised just like virgin rubber. In addition to this ultrasonic devulcanisation technique, there are several surface modifications, which are possible on the latex waste. Chemical [20,21], mechanical [22,23], plasma [24,25], corona [26,27] and electron beam radiation [28,29] are reported to be useful to improve the matrix filler adhesion. Epoxidised natural rubber or ENR is a relatively new rubber, having properties similar to those of synthetic rubbers rather than natural rubber. It has low air permeability [30] (comparable to that of butyl rubber), good oil resistance [31] (comparable to that of nitrile rubber) and good dynamic properties. It exhibits strain-induced crystallisation [32] similar to natural rubber.

In this article, we evaluate the effects of using powdered latex rejects as filler in ENR. The influence of filler loading on the curing characteristics is discussed. Also, the effect of both particle size and loading of the filler on the mechanical properties, swelling and failure behaviour are compared and presented. A comparative study based on the mode (conventional and efficient) of the vulcanisation system and its effect on the tensile strength of the vulcanisates also is carried out. The dependence of filler–ENR matrix adhesion on the particle size of the filler also is examined on the basis of sulphur migration phenomena. Several theoretical models have been used to fit the experimental tensile modulus values. The filler particle morphology, filler dispersion and filler–matrix interphase adhesion are analysed using scanning electron microscopy.

2. Experimental

2.1. Materials

The basic material used in this work is ENR-25, epoxidised natural rubber having 25% epoxidation, manufactured and supplied by the Rubber Research Institute of India, Kottayam, India. Its composition is given in Table 1. NR latex filler was prepared from WLR, supplied by Hindustan Latex Ltd, Thiruvananthapuram, Kerala, India. Other compounding ingredients such as zinc oxide, stearic acid and CBS (*N*-cyclohexyl benzthiazyl sulphenamide) were of reagent grade and obtained from local rubber chemical suppliers. Toluene (reagent grade) was used for carrying out swelling studies.

2.2. Methods

2.2.1. Preparation of powder rubber

The ground vulcanisate preparation was done in a fast-rotating toothed-wheel mill. The advantage of this technique is that one can obtain a fine elastic rubber powder, unlike cryoground rubber (CGR), which is stiff [33]. Therefore, CGR will not permit easy diffusion of curatives into it. The powder rubber was found to be polydispersed in particle size. It was then sieved into four different particle sizes, ranging from 0.3 to 0.5 mm (size 1 or S1), 0.6 to 0.9 mm (size 2 or S2), 1.7 to 2.5 mm (size 3 or S3) and 9 to 11 mm (size 4 or S4). A mill-sheeted form (M) of the latex rejects also was prepared by passing the rejects through a hot two-roll mill for 10 min. Various particle sizes and mill-sheeted form of the filler are presented in Fig. 1.

2.2.2. Mixing, rheometry and preparation of test samples

Mixing of ENR and filler were carried out using a laboratory size two-roll mixing mill having a friction ratio 1:1.4, as per ASTM D 15-627. The recipe used is given in Table 2. The effect of addition of up to 40 phr of latex filler in ENR is investigated, with emphasis on the size of the filler and its influence on sulphur migration.

The cure characteristics of the mixes were determined using a Monsanto Rheometer model R-100 at 150°C by

Table 1
Composition of ENR-25

Constituent/properties	%/Value
Epoxy content (%)	25
Density (gm/cc)	0.97
Mooney viscosity	80–90
Protein content (%)	0.001–0.0004
Molecular weight	10^5
Colour	Yellow

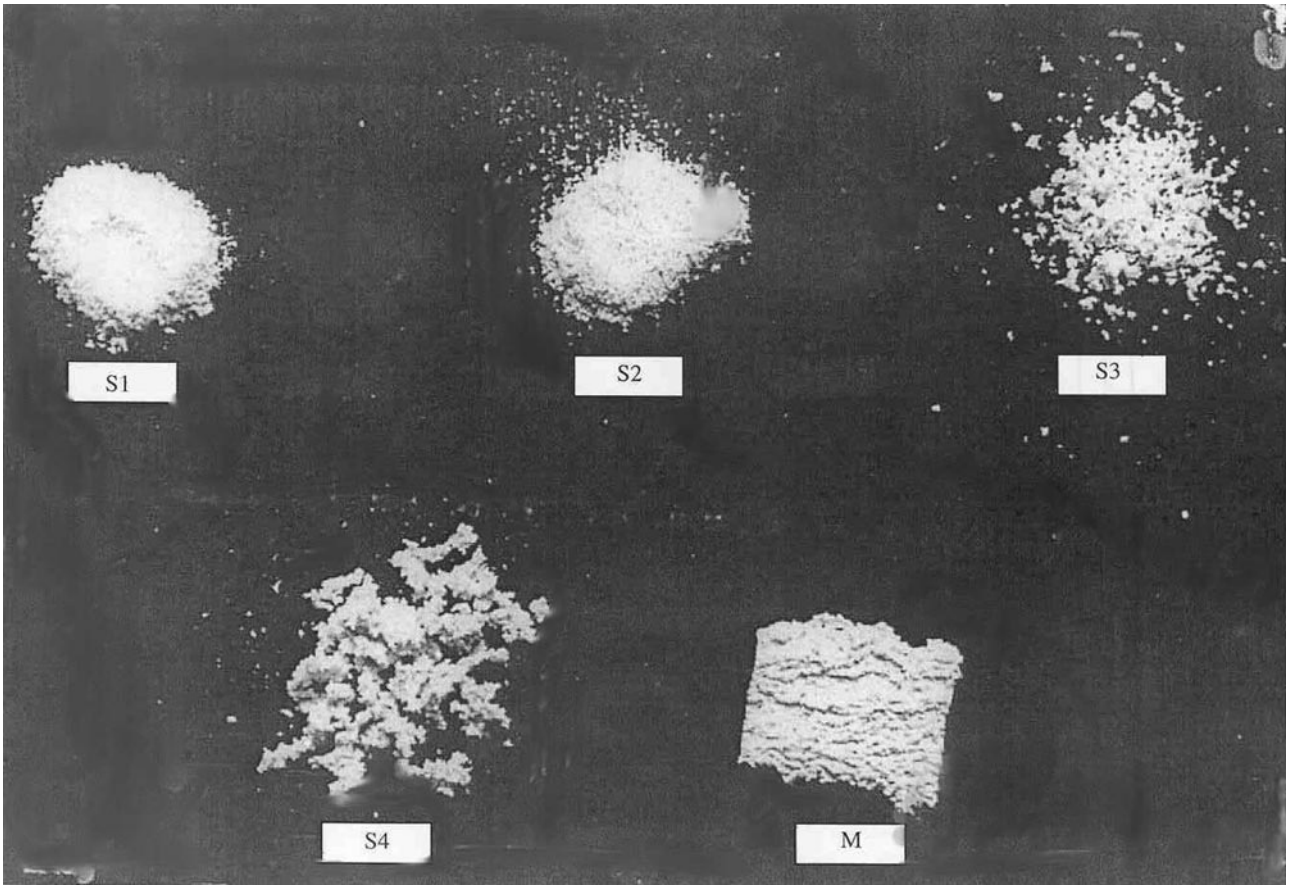

Fig. 1. Different particle sizes (sizes 1–4) and mill-sheeted form of the filler.

measuring the optimum cure time, scorch time and induction time. The kinetics of vulcanisation [22] was also studied from the rheographs and correlated with cure rate index values.

The compounds were then compression-moulded at 150°C using an electrically heated hydraulic press for their respective cure times (t_{90}). Dumbbell-shaped tensile and angular tear specimens were punched out from the compression-moulded slabs along the mill grain direction.

2.2.3. Physico-mechanical testing of the samples

Stress–strain was determined on an Instron Universal Testing Machine, using a C-type dumbbell specimen, according to ASTM D 412-80. The tear strength was determined as per ASTM D 624-81 using angular tear specimens. Both the tests were done at 28°C and at a cross-head speed of 500 mm/min.

Table 2
Base formulation

Material	Control (phr)
ENR-25	100
Zinc oxide	5
Stearic acid	2
CBS	0.6
Sulphur	2.5
Calcium stearate	1
WLR	Variable (0,10,20,30,40)

2.2.4. Swelling studies

Equilibrium swelling [34] measurements of the vulcanisates was performed in toluene at room temperature. The samples were allowed to equilibrate for 7 days and again the solvent was renewed after 3 days, to remove soluble materials from the vulcanisates. The variation of cross-link density with filler loading was analysed. In order to assess the ENR matrix–filler interaction previously established, Kraus [35], Cunneen and Russell [36] and Lorenz–Park [37] models were applied.

2.2.5. Sulphur diffusion studies

The sulphur migration phenomena that takes place between ENR and the filler phases was studied using a three-layer model [38] (Fig. 2) system. It consists of three layers, one layer of NR latex waste (all sizes 1–4 and M were tried) was sandwiched between two layers of gum ENR compounds. In one half of the specimen, the outer ENR layers were separated from the inner latex waste layer by using aluminium foils (non-contact surface) and

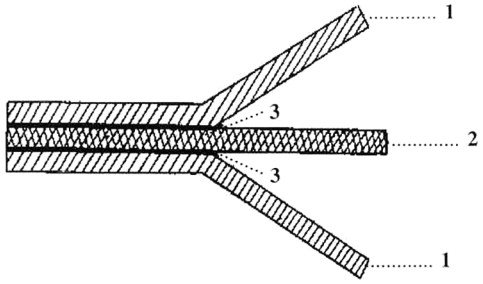

THREE LAYER MODEL

1. GUM ENR MATRIX
2. NR LATEX WASTE
3. ALUMINIUM FOIL

DIMENSIONS OF THE SAMPLE

	LENGTH (cm)	BREADTH(cm)	THICKNESS (cm)
1. GUM ENR MIX	16	8	0.2
2. NR LATEX WASTE	16	8	0.2
3. ALUMINIUM FOIL	8	8	0.004

Fig. 2. Model to analyse sulphur migration.

in the other half, the aluminium foil was omitted (contact surface). The system was then subjected to vulcanisation at low pressure. Then the middle layer was separated. The cross-link density and swelling index values of this layer were determined by swelling the samples taken from the contact and non-contact regions. If sulphur migration occurs from the outer ENR matrix to the middle latex waste layer, the cross-link density of the latex waste layer at the contact surface will be increased. The extent of increase will be a direct measure of extent of sulphur migration.

2.2.6. Scanning electron microscopic studies

The SEM observations of filler morphology and distribution were made in a direction transverse to the grain direction, using a JEOL JSM-35C model scanning electron microscope. Fracture surfaces of the test samples were carefully cut from the failed test pieces without touching the surfaces. These specimens were sputter coated with gold, within 72 h of observation.

3. Results and discussion

3.1. Processing characteristics

The powdered filler particles are found to be almost spherical in shape with fissured surfaces (Fig. 3). Since particles of larger diameter also can penetrate through the meshes because of their elasticity, the particle size data can be presented as distribution curves (Fig. 4). The distribution broadens as we go from sizes 1 to 4. The average size and most frequent size range are given in Table 3. The number average (D_n) and weight average (D_w) diameters are calculated using the equations given below and are also presented in Table 3.

$$D_n = \sum N_i D_i / \sum N_i \quad (1)$$

$$D_w = \sum N_i D_i^2 / \sum N_i D_i \quad (2)$$

where N_i is the number of rubber particles having a certain diameter D_i.

It is clear from the table that all these parameters show an increase from size 1 to size 4. The shape factor p and its significance will be discussed later.

The processability characteristics of the compounds (Table 4) can be studied from the rheographs. The finest size filler (size 1) is selected for the determination of processing/curing characteristics. The minimum torque in the rheograph is a measure of filler content in the rubber and is presented as the minimum viscosity value M_n. These values first register an increase with increase in filler content, but later they decrease (Table 4). The initial increase is due to the presence of cross-linked rubber

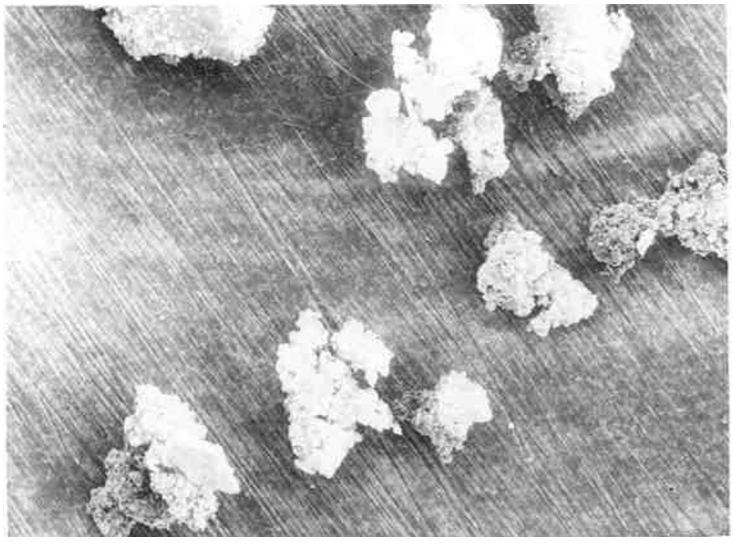

Fig. 3. Scanning electron micrograph of powdered rubber rejects.

particles in ENR and the decrease at 40-phr loading may be because of the higher extent of mastication during mixing. The maximum torque in the rheograph is a measure of cross-link density in the rubber and is presented as the maximum viscosity value M_h. It is found that the presence of particulate inclusions increases the maximum torque. However, in our case, where the inclusion itself is a rubber, the variation may be a result of the combined effect of cross-link density variation and the presence of cross-linked particles. At 10-phr loading, the presence of cross-linked particles increases M_h, but at later stages of loading, the sulphur migration (which will be discussed later) becomes predominant, which leads to reduced cross-link densities. This causes the reduction in M_h values.

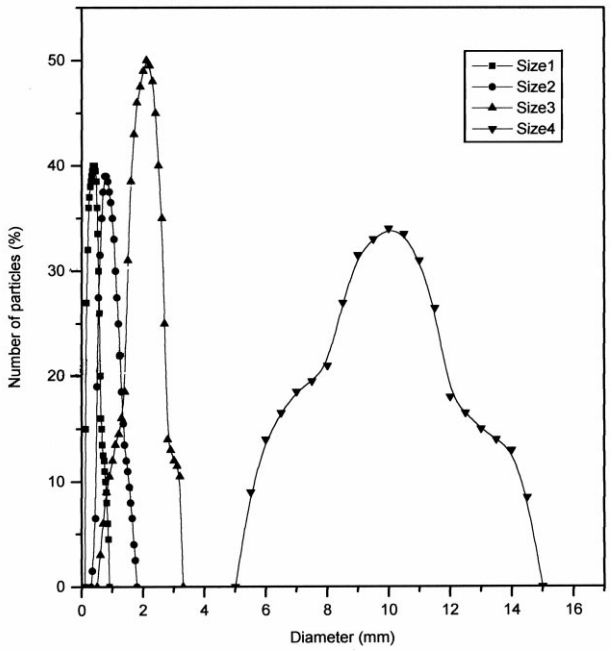

Fig. 4. Particle size distribution curves.

As the filler content increases, the optimum cure time, t_{90} (time needed for the formation of 90% cross-links), scorch time t_2 (premature vulcanisation time) and induction time t_1 (time to start the vulcanisation process) are found to decrease. These results are presented in Fig. 5. This is due to the presence of unreacted accelerator zinc diethyldithiocarbamate (ZDEC) in the latex waste. ZDEC is one of the important accelerators currently used in the manufacture of condoms. Its structure is shown in Fig. 6a. In order to confirm its presence we have extracted the unreacted ZDEC from the latex waste, and it has been evaluated by IR. The spectrum is presented in Fig. 6b. The peaks at 700–600 cm^{-1} are due to C–S stretching and that at 790–770 cm^{-1} indicates the presence of ethyl chain ($-CH_2-CH_3$). The C=S stretching peak is visible at 1250–1020 cm^{-1} and the peak at 2820–2760 cm^{-1} indicates the presence of $N-CH_2$ group in the compound. All these confirm the presence of unreacted accelerator in the latex rejects. Therefore, it is clear that the rubber compound contains the accelerator CBS (*N*-cyclohexyl benzthiazyl sulphenamide) added in the formulation (Table 2) and the unreacted accelerator ZDEC, already present in the latex rejects. As a result of the combined accelerating effect, the three parameters, namely t_{90}, t_2 and t_1, decrease with loading of filler.

The increase in speed of the curing reaction with filler loading can be analysed systematically, by calculating two parameters, namely the cure rate index (CRI) and reaction rate constant (k). The cure rate index values (CRI) are calculated using the equation:

$$\mathrm{CRI} = 100/t_{90} - t_2 \quad (3)$$

Table 3
Particle size data

Particle size	Average size (mm)	Most frequent size range (mm)	No. average diameter (mm)/D_n	Wt. average diameter (mm)/D_w	Shape factor p
Size 1	0.5	0.3–0.5	0.401	0.489	2.2951
Size 2	1.05	0.6–0.9	0.961	1.083	2.0067
Size 3	1.9	1.7–2.5	2.11	2.34	2.1667
Size 4	10	9–11	10.09	10.72	1.6513

where t_{90} is optimum cure time and t_2 is rheometric scorch time.

CRI values are given in Table 4 and its variation with filler loading will be discussed later. The kinetics of cure reaction is analysed by the method [22] explained below.

The general equation for the kinetics of a first-order chemical reaction can be written as:

$$\ln (a - x) = -kt + \ln a \quad (4)$$

where a is the initial reactant concentration, x is the reacted quantity of reactant at time t and k is the first-order reaction rate constant.

The rate of cross-link formation during the vulcanisation of rubber is usually monitored by measuring the developed torque. Since these torque values are a direct measure of the modulus of the rubber, the following substitutions can be made.

$$a - x = M_\infty - M \quad (5)$$

$$a = M_\infty - M_0 \quad (6)$$

where M_∞ is the maximum modulus, M_0 is the minimum modulus and M is the modulus at time t.

Substitutions of torque values for modulus give the equations:

$$a - x = M_h - M_t \quad (7)$$

$$a = M_h - M_0 \quad (8)$$

where M_h is maximum torque, M_0 is minimum torque and M_t is the torque at time t.

The plots of $\ln (M_h - M_t)$ versus time, t, are presented in Fig. 7. Even though linearity is claimed for the plots theoretically, deviations from linearity are experimentally observed for certain points. The observed linearity in the plots confirm that the cure reaction of the samples follow first-order kinetics. The slope of the respective straight lines gives the cure reaction rate constant (k) and are presented in Table 4.

It is clear from Table 4 that both CRI and k values show an increase up to 30-phr latex waste loading and later they decrease at 40-phr loading. The initial increase is again due to the presence of unreacted accelerator in the latex waste. This cure-activating nature of latex filler is an advantage, since a faster curing sample will have a high production rate. However, this cure activation is found to level off at higher loadings of latex waste. Since the filled ENR compound is more stiff and non-tacky, the compound is easy to handle for further processing. On the other hand, the unfilled ENR is very tacky, making it difficult to handle.

3.2. Mechanical properties

The mechanical properties of elastomers filled with powder rubber depend on many factors, such as the following.

(i) Strain crystallising nature of the filler.
(ii) Adhesion [39] of the filler with matrix.
(iii) Particle size of the filler.
(iv) Extent of sulphur migration from matrix to filler phase, which is controlled by many factors such as:
  (a) The concentration of polysulphidic linkages in the matrix and filler. If the concentration of polysulphidic linkages in the matrix is higher than that of filler, sulphur migration will be less, but it will be extensive if the reverse is true [22].
  (b) The particle size of the filler. As the particle size of the filler decreases, the contact surface area with the ENR matrix increases, leading to more sulphur diffusion.

As the filler content increases, the tensile strength (Fig. 8)

Table 4
Cure characteristics

Loading (phr)	Minimum viscosity (M_n) ($dN - m$)	Maximum viscosity (M_h) ($dN - m$)	Cure rate index (CRI) (min^{-1})	Rate constant (k) (min^{-1})
0	3	35	12.5	0.266
10	4	44	33.3	0.631
20	4.5	44	33.3	0.675
30	6	43	36.4	0.810
40	4	42	32.1	0.800

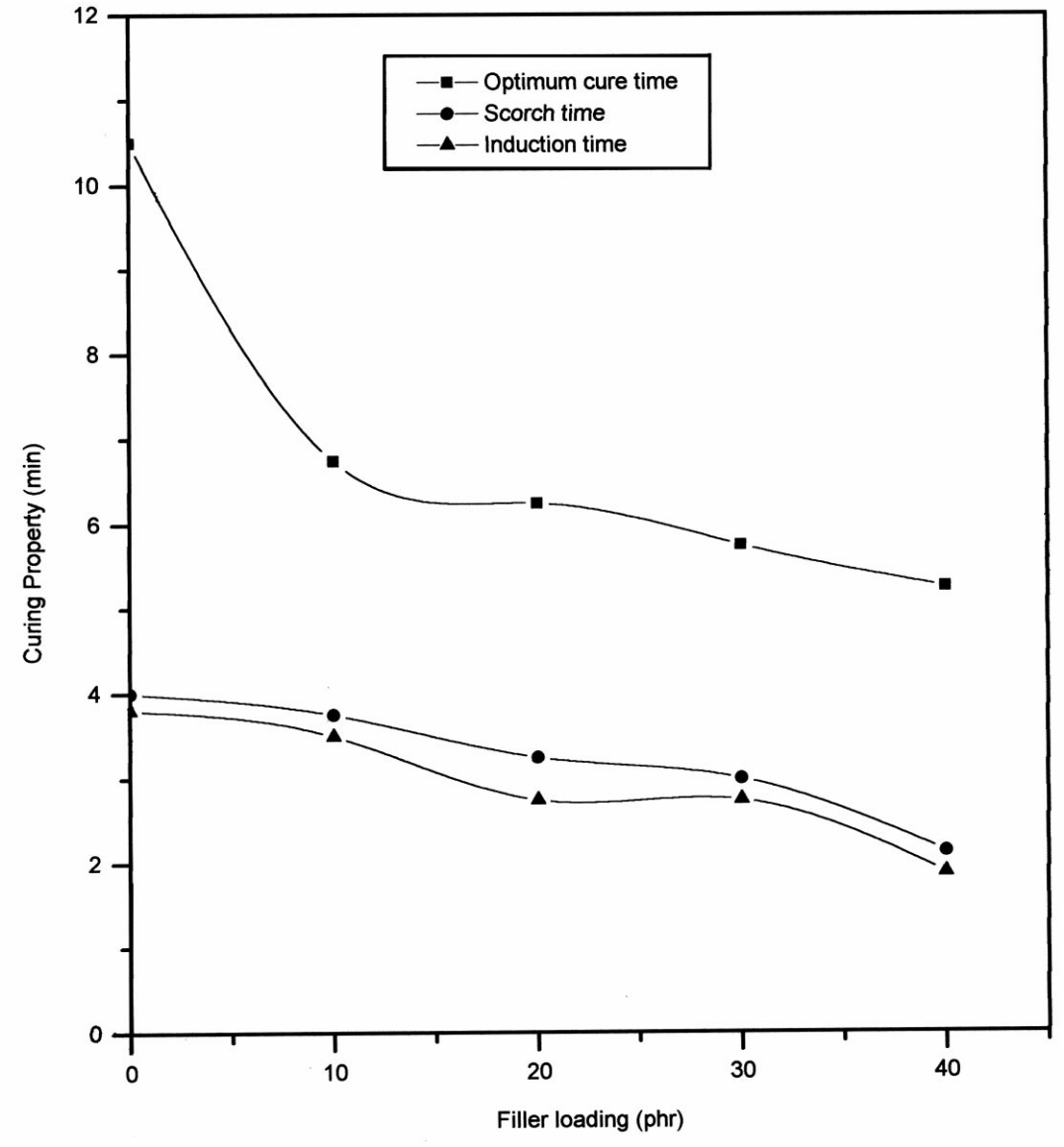

Fig. 5. Effect of filler loading on curing characteristics.

increases dramatically and reaches a maximum value at 30-phr loading. Beyond 30-phr loading, the tensile strength values show a decrease or levelling-off behaviour. For size 1, the increase is about 300%. The increase in tensile strength is due to the strain crystallising nature of NR latex filler particles. The threshold value of strain, required for strain crystallisation of natural rubber (NR), is 500%. Since the filler particle is very small, it will cover this value even at the initial stages of extension. The increase in tensile strength with loading confirms the fact that NR retains its strain crystallising nature, even if it is in the form of fine filler. Lewis and Nielsen [40] postulated that as the particle size decreases, the contact surface area increases, providing a more efficient interfacial bond, leading to better properties. At high filler loading, there will be an increased tendency for agglomeration, which may weaken the interfacial bonds. It is also important to mention that the tendency for agglomeration increases with the decrease of particle size. At 40-phr loading of size 1 filler, the latter effect exceeds the former and, therefore, tensile strength drops suddenly. Such a sharp drop is noted only for size 1. Agglomerates as described above, tend to contain voids, so that their apparent volume will be considerably greater than their true volume. If the agglomerates are hard with appreciable strength, then the filled material will have a higher strength than expected. Soft disintegrated agglomerates, however, as in the present case, produce a reverse effect, which manifests as a sharp drop in tensile strength at higher filler loading. Since such an agglomeration is less probable for higher particle sizes, a sharp drop in tensile strength is not observed.

We have noted many interesting behaviours associated with the particle size–performance relationship. In the case of fine filler, the contact surface area with the matrix is more. This can lead to enhanced sulphur migration from

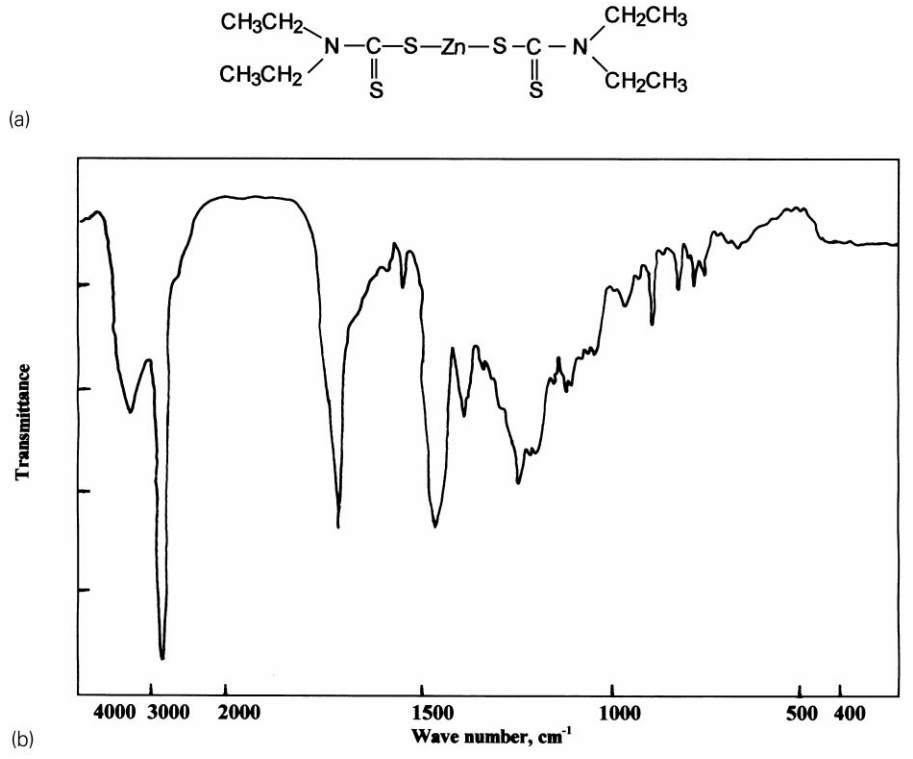

Fig. 6. (a) Structure of unreacted accelerator (ZDEC). (b) IR spectrum of unreacted accelerator (ZDEC).

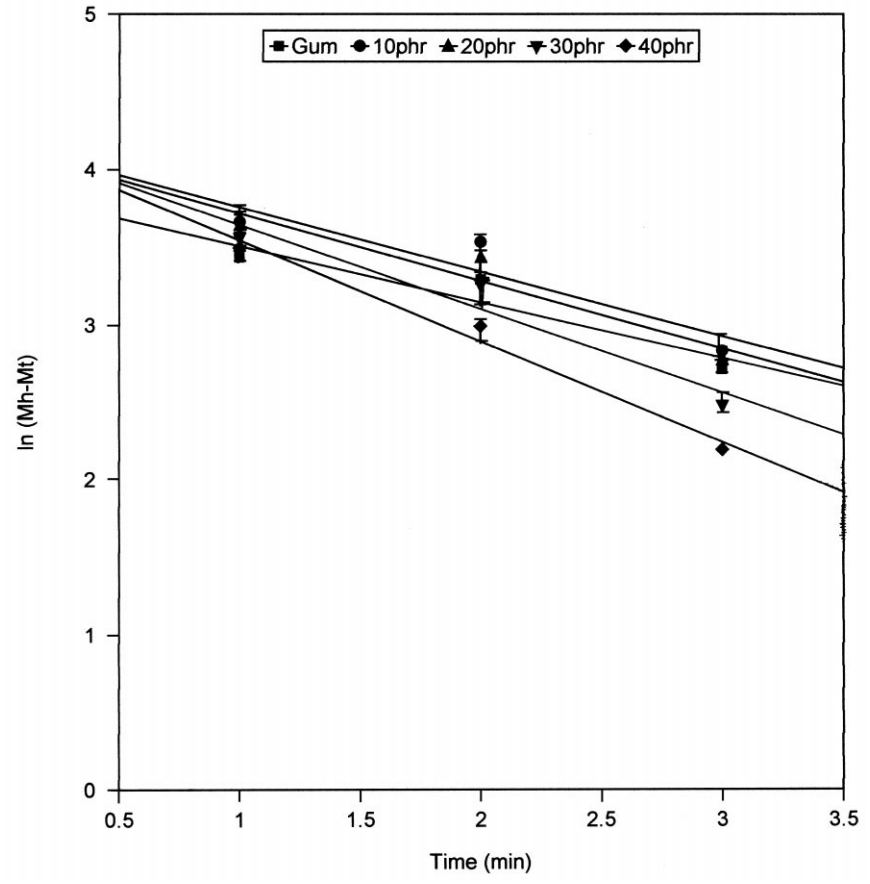

Fig. 7. Plots of ln ($M_h - M_t$) vs. time, t.

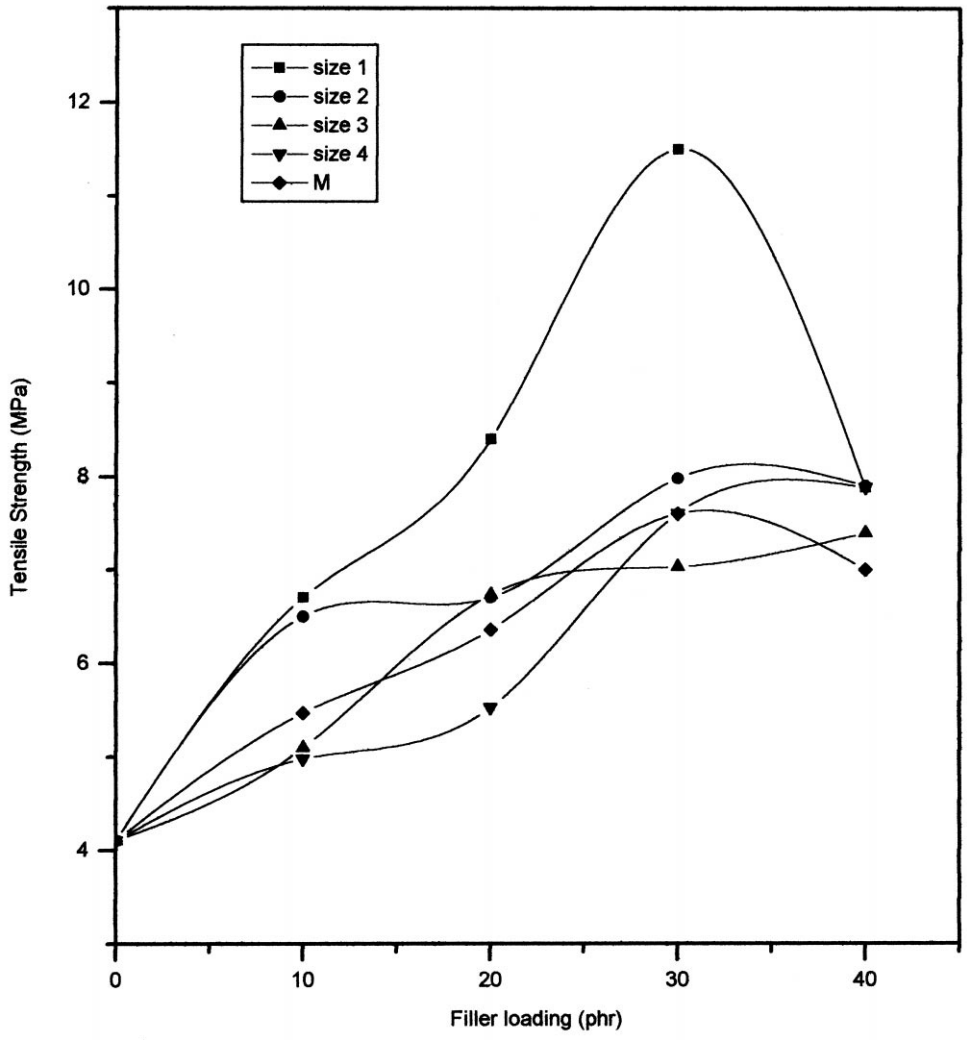

Fig. 8. Effect of filler loading and size on the tensile strength of ENR cross-linked by a CV system.

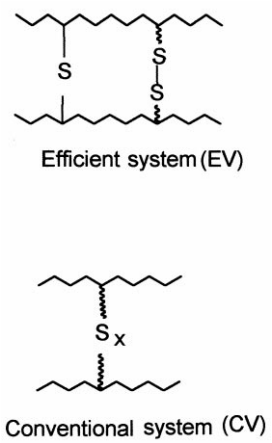

Fig. 9. Schematic sketch of sulphur linkages for different vulcanisation systems.

matrix to filler and worsening of tensile properties. So one expects inferior properties for ENR filled with size 1 filler. According to our studies, however, size 1 filler is found to be superior (Fig. 8). This is mainly because fine particles of size 1 will have a uniform distribution, which makes an efficient stress transfer possible. The second reason is the competition between polysulphidic linkages in the ENR matrix and filler. The basic formulation used here is a conventional vulcanisation (CV) system with high sulphur-to-accelerator ratio (Table 2). This provides a higher concentration of polysulphidic linkages in ENR, than that of the filler. A schematic sketch of the CV system is given in Fig. 9. When the concentration of polysulphidic linkages in the matrix is higher than that of the filler, sulphur migration from the matrix to the filler is less predominant [22]. Therefore, the tensile properties for fine fillers (sizes 1 and 2) become superior to those of large-size fillers (sizes 3, 4 and M).

In order to analyse this effect in detail, we have tried a recipe with a low sulphur-to-accelerator ratio

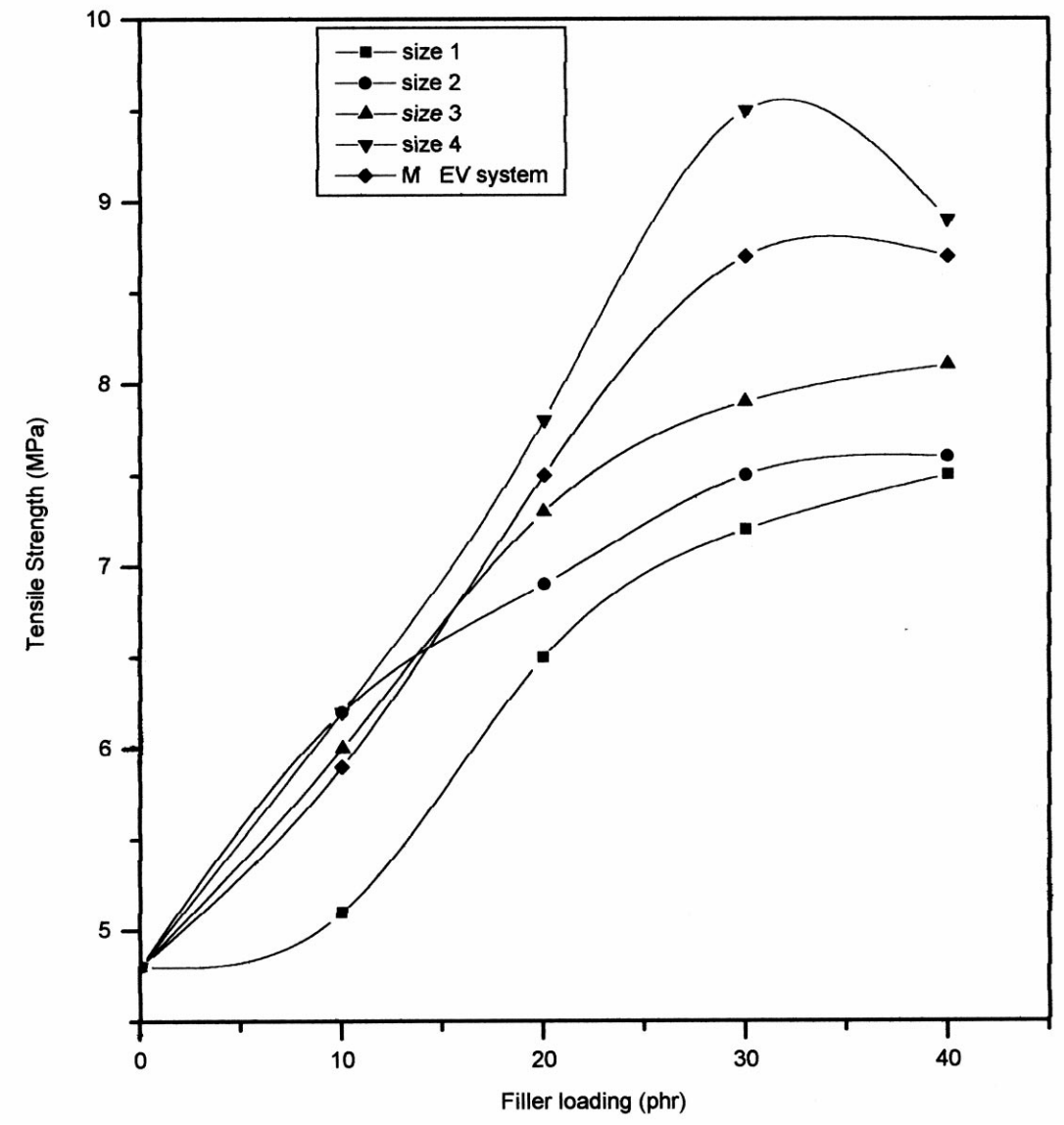

Fig. 10. Effect of filler loading and size on the tensile strength of ENR cross-linked by an EV system.

Table 5
Cross-link density values from sulphur migration studies

Vulcanisation system	Filler size	Cross-link density values $\times 10^{-5}$ (gm moles/cc) of middle layer	
		Contact surface (CS)	Non-contact surface (NCS)
CV	S1	1.14	1.18
	S2	1.16	1.15
	S3	1.15	1.14
	S4	1.15	1.16
	M	1.13	1.14
EV	S1	1.45	1.21
	S2	1.30	1.22
	S3	1.31	1.23
	S4	1.20	1.23
	M	1.25	1.24

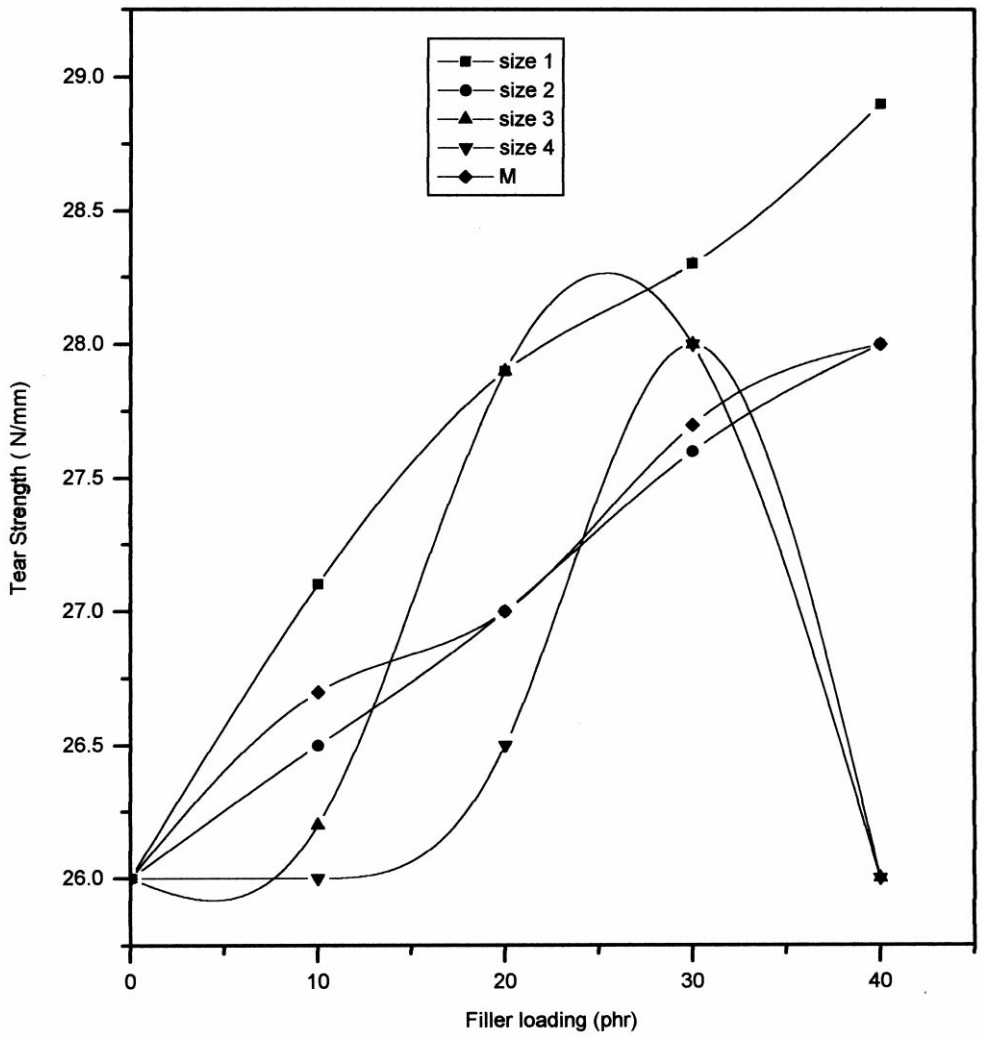

Fig. 11. Effect of filler loading and size on the tear strength of ENR vulcanisates.

(sulphur — 0.5 phr, CBS — 1.5 phr). This efficient vulcanisation (EV) system provides mainly mono and disulfidic linkages in the ENR matrix phase (Fig. 9). Here, since the concentration of polysulphidic linkages in the filler is more than that of the matrix, sulphur migration is extensive and is maximum in the case of size 1 (owing to the large contact area). Therefore, the tensile strength values for large-size fillers (sizes 4 and M) become higher than that of size 1. This is clear from Fig. 10. There is one more important reason for the superior properties of large-size fillers, mainly size 4. It is clear from Fig. 4 that the size 4 filler has the widest particle-size distribution. Such mixtures of particles with differing sizes can pack more densely than monodispersed particles because smaller ones can fill the interstitial spaces between the closely packed large particles to form an agglomerate. Such an agglomerate [41], which is formed from a polydispersed or ungraded system may be able to carry a large proportion of load and is, therefore, superior to the agglomerate discussed earlier. Such cases describing the superior performance of large particles were already reported by many researchers [42].

The absence of sulphur migration in the CV system as well as its presence and extent in the EV system is confirmed by using a three-layer model as shown in Fig. 2. The dimensions of the model are also shown in Fig. 2. For the CV system (Table 5), the cross-link density of the sample obtained from the contact surface of the middle latex waste layer is found to be almost the same as that from the non-contact surface. Moreover, the values are found to be similar for all the particle sizes of the filler. This data confirms the absence of sulphur migration in the CV system. Whenever sulphur migration is present in the system, the cross-link density of the sample from the contact surface must be higher than that of the non-contact surface. Owing to the higher concentration of polysulphidic linkages in the ENR matrix for the CV system, sulphur migration must be less and consequently, the cross-link density from the contact and non-contact surfaces must be comparable.

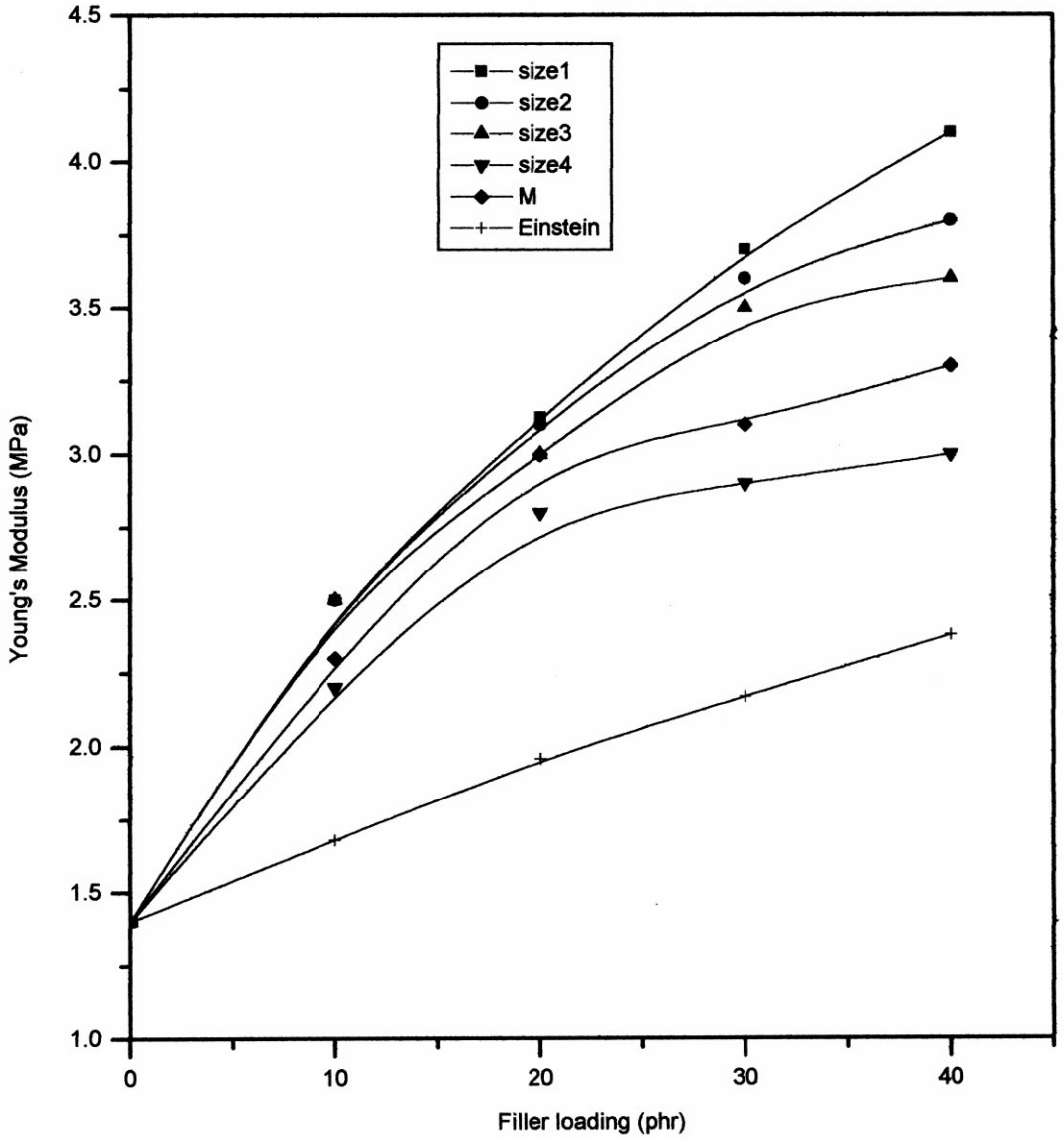

Fig. 12. Comparison of the experimental data with Einstein's model for a CV system.

This is found to be true for the present case. However, for the EV system with lower concentration of polysulphidic linkages in the ENR matrix, the sulphur migration must be predominant and consequently, the cross-link density from the contact surface must be higher than that from the non-contact surface. However, various additional factors, such as the differential swelling of prophylactic particles and the ENR matrix, the competition between the interaction parameters of the two polymers and the overall compact structure of the system deciding the diffusion characteristics, make the swelling results a bit irregular. The superior influence of the compact nature of the polymer matrix over the interaction parameter values on the swelling process will be discussed in a later section. Even in the case of the EV system, the cross-link density of the sample from the contact surface is found to be only slightly higher than that from the non-contact surface. Even though this proves the presence of sulphur migration, this factor alone is unable to support the observed changes in mechanical properties.

The tear strength of gum and filled ENR samples are presented in Fig. 11. With increase in loading of the filler, there is slight improvement in the tear strength of the samples up to 30-phr loading. This increase is due to the restriction in the advancement of the tear front. This restriction is caused by the elongation of filler particles in the tear path. The performance of size 1 filler is superior here. In the case of finer filler (size 1) there will be a large number of filler particles present per unit area to elongate to high strains and to resist tear propagation. As the particle size increases to sizes 2 and 3, the tear strength decreases and the values are minimum for size 4. However, at 40-phr loading, the value either drops or levels off for large filler sizes.

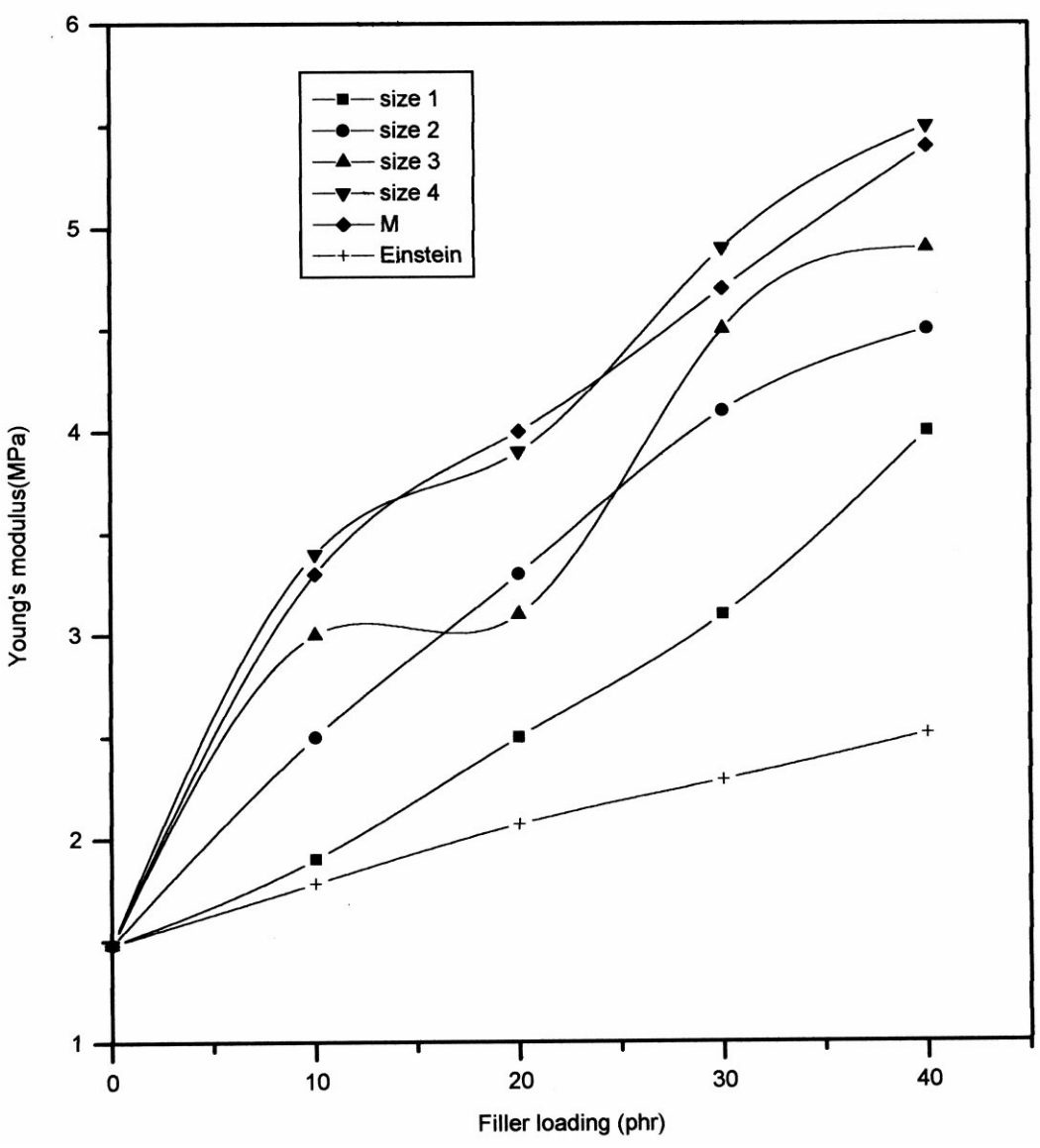

Fig. 13. Comparison of the experimental data with Einstein's model for an EV system.

3.3. Theoretical modelling of Young's modulus

Young's modulus of particulate-filled composites can be predicted using several theoretical models. Even though a large number of theoretical equations are generally available for composite materials, only a few are specially formulated for composites with non-rigid matrices. These include the Einstein, Mooney, Guth, Cohan, and Brodnyan models. The Einstein equation and its modifications are usually applied to predict the modulus of the composites containing rigid fillers such as black and silica. These theories are applied to systems with non-rigid fillers such as prophylactic particles, which undergo strain crystallisation on stretching.

The simplest theoretical equation for the reinforcement of a material with a filler is given by Einstein [43]. The equation is

$$M_c = M_m(1 + 2.5V_f) \quad (9)$$

where M_c is Young's modulus of the composite, M_m is Young's modulus of the matrix and V_f is the volume fraction of the filler. The Young's modulus values of all the four particle sizes and mill-sheeted form of the latex waste filler are correlated with the Einstein model in Figs. 12 and 13. Fig. 12 represents the conventional vulcanisation system, where the finest filler (size 1) is most reinforcing. Therefore, it presents a plot that is far above that given by the Einstein equation. It is a general observation from the figure that only large-size fillers such as sizes 3 and 4 are found to give close values to that of Einstein. With increasing loading of fillers, the deviation shown by the finer-size fillers such as sizes 1 and 2 goes on increasing, while that of large-size fillers

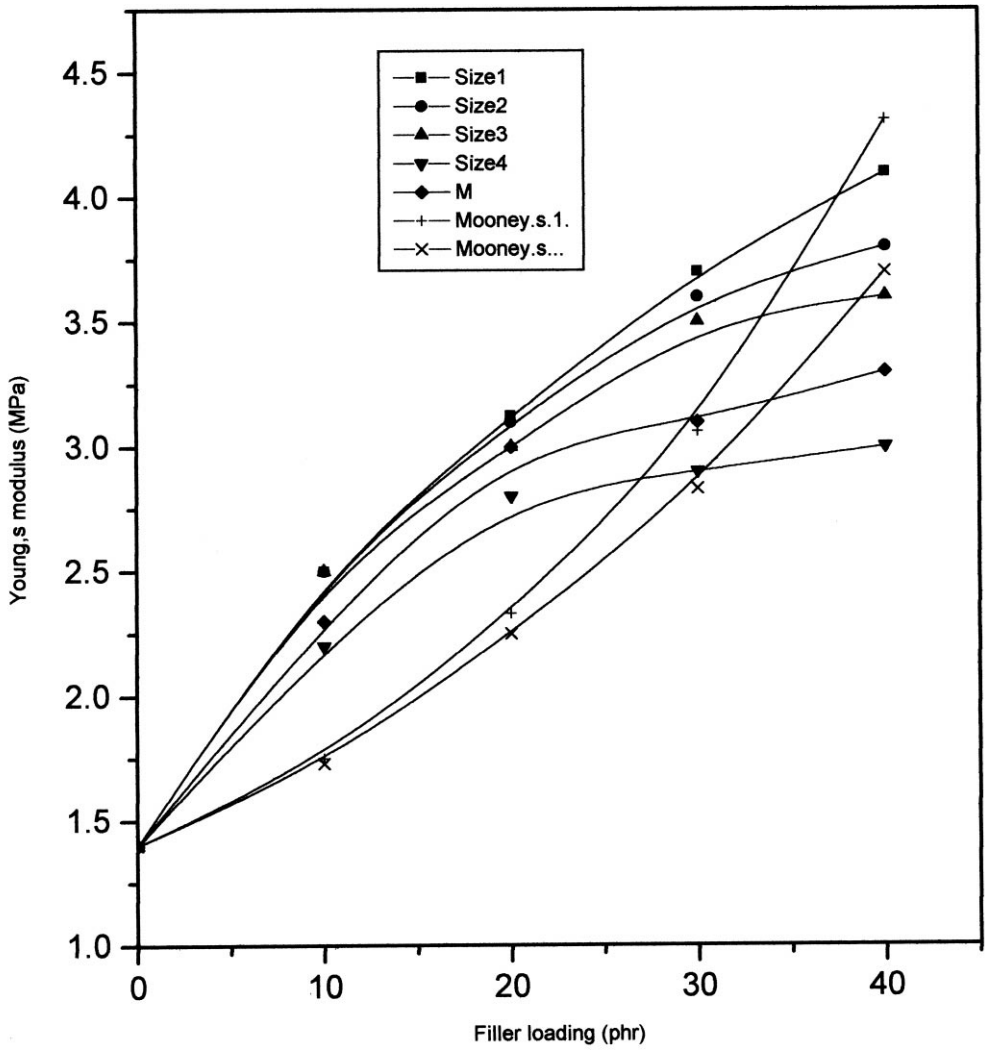

Fig. 14. Comparison of the experimental data with Mooney's model for a CV system.

(sizes 3 and 4) decreases. The behaviour shown by the mill-sheeted form (M) is in between finer- and large-size fillers.

Fig. 13 represents the Young's modulus correlation of all filler grades with the Einstein model, in an EV system. Here, the finest filler (size 1) is weakly reinforcing and, therefore, its plot is closer to that of Einstein, mainly at 10-phr loading. It is found that as the particle size increases to sizes 2–4, the deviation of the modulus values from those of the model increases. Also, as the loading increases, the magnitude of deviation also increases even though some irregularities are observed for the size 3 filler at 20-phr loading. It is a general observation that for CV and EV systems, none of the filler grades shows an exact correlation with the Einstein model.

The observed deviations from the model are due to the following reasons:

(1) The Einstein model assumes that the stiffening action of a filler is independent of its size, while it has already been established by many researchers [44] and also by our studies [45] that the reinforcement of the matrix by a filler changes with its particle size. Since this effect is not accounted for by the model, the experimental values for different size grades deviate differently from the model.

(2) The model assumes that the filler particles are spherical in shape and there is perfect adhesion between the filler and matrix. It is clear from the SEM photos of filler particles (Fig. 3) that the filler particles have non-uniform size distributions and shape. Also, we have noted from the scanning electron micrographs (Fig. 28a and b) that the filler particles are not firmly bonded to the matrix. The presence of an air pocket over the filler particles has already been confirmed by the work of Phadke et al. [46]. Therefore, the imperfect adhesion between filler and matrix also contributes to the observed deviations from the model.

(3) It is stated by Mooney [47] that the Einstein equation is valid only for low concentrations of filler. This is because at higher filler loading, the strain fields around filler particles can interact, causing deviations from the model.

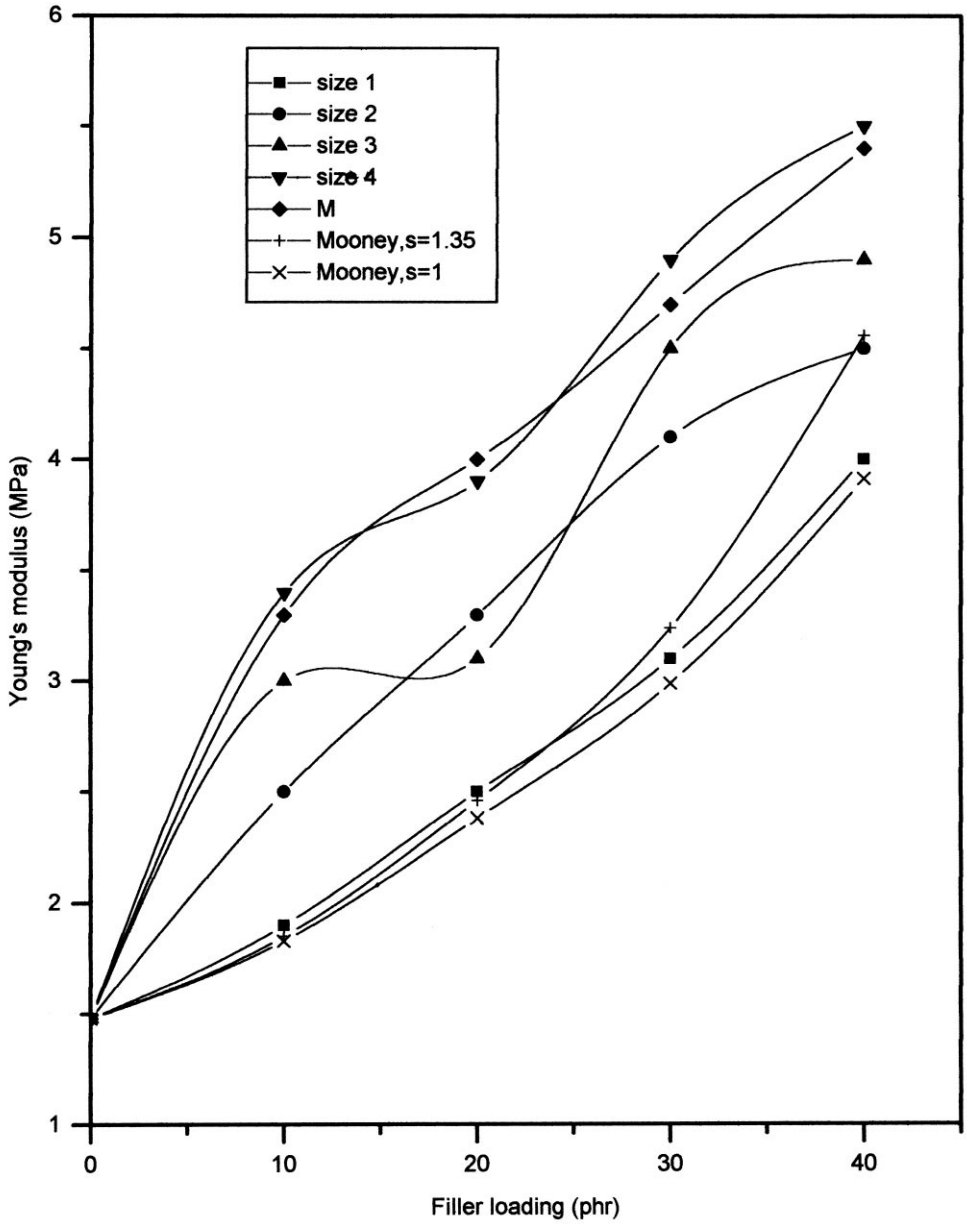

Fig. 15. Comparison of the experimental data with Mooney's model for an EV system.

(4) The final and most important reason for the deviation may be the lower rigidity of the filler compared to normal fillers such as carbon black or silica. Since it is assumed in the Einstein model that the filler is much more rigid than the matrix, this factor may cause a number of secondary reasons for deviations from the model. However, it has already been proved by Smallwood in the literature [48] that the Einstein equation is more useful for predicting the elastic behaviour of rubbers containing non- or less-reinforcing fillers. The correlation, even though less, between experimental and theoretical values observed in our case again proves this fact.

The Einstein equation does not account for the particle agglomerations. Therefore the equation has been modified by Mooney [47] by introducing a crowding factor *S*. The Mooney equation is given as;

$$M_c = M_m \exp\{2.5V_f/1 - SV_f\} \quad (10)$$

where M_c, M_m and V_f are the same as explained earlier. *S* is the crowding factor or relative sedimentation volume of the filler, which accounts for the agglomeration of filler particles. Agglomerates of filler particles tend to contain voids or air spaces so that their apparent volume will be higher than their true volume. *S* is defined as the ratio of apparent volume occupied by the filler to its true volume.

According to Mooney [47], the minimum possible value that *S* can have is unity while its experimental value ranges

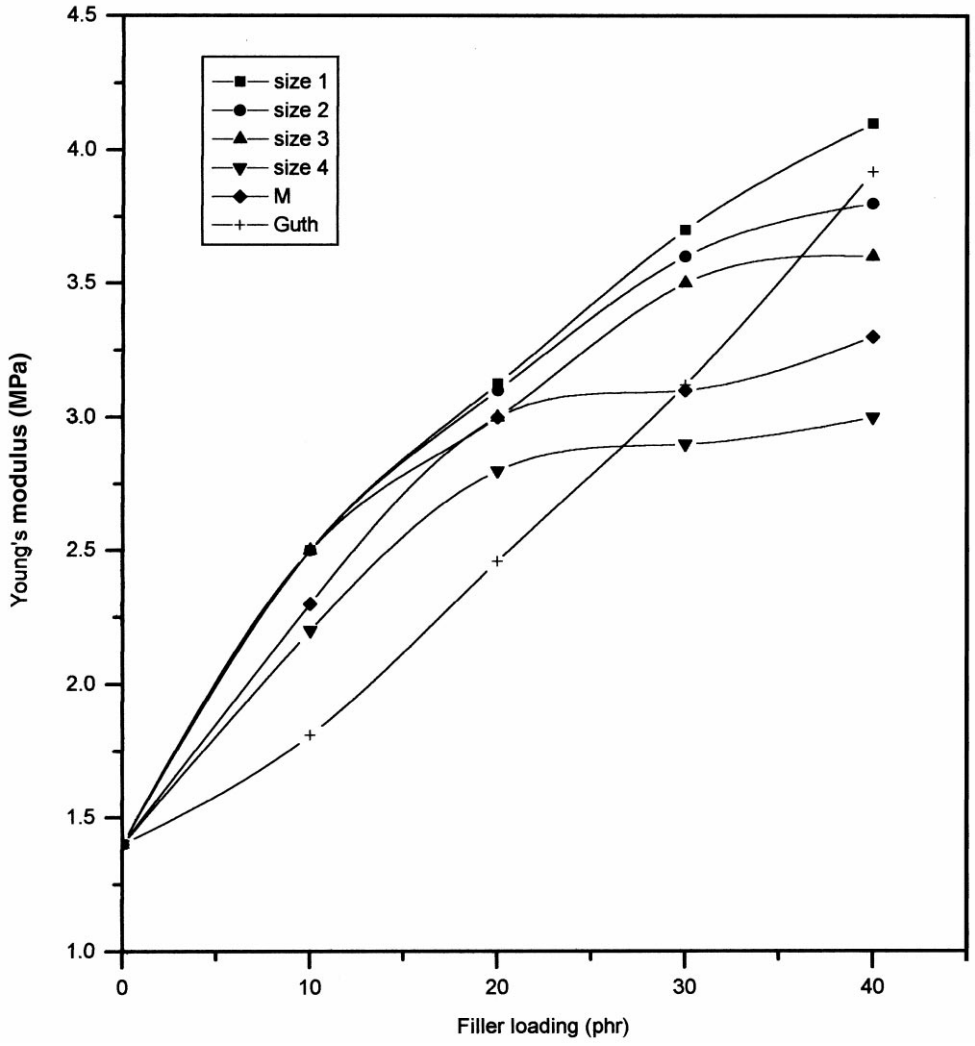

Fig. 16. Comparison of the experimental data with Guth's model for a CV system.

from 1.2 to 2. However, it has been reported [49] that up to $V_f = 0.5$, a value of 1.4 (or 1.35) can fit the best experimental values. For our system, we have made our calculations using two values of S, 1.35 and 1. Fig. 14 is the Mooney model fitting curves of different size grades of latex waste filler, in the conventional vulcanisation system. When the value of S is 1.35, the size 4 filler gives comparatively closer values than that given by the equation at 10- and 20-phr loading. However, as the loading increases to 30 phr, a better value is shown by the mill-sheeted form, while the size 4 filler gives a value below that of the model. All other filler sizes such as 1, 2 and 3, deviate greatly from the model mainly at lower loadings. As the filler loading increases to 40 phr, the model plot shoots up and, therefore, closer values are shown by finer filler sizes 1–3. Size 4 and mill-sheeted form values lie much below that of the model at highest loading. When the value of S is 1, the size 4 filler gives better agreement mainly at 30-phr loading and sizes 2 and 3, at 40-phr loading. Large-size fillers, size 4 and the mill-sheeted form, are below that of the Einstein model while finer sizes 1 and 2 are above. As far as the efficient vulcanisation system (Fig. 15) is concerned, for $S = 1.35$, the size 1 filler is closer to the values predicted by the Mooney equation. This is due to its weakly reinforcing nature in the EV system. Most other size grades and mainly sizes 4 and the mill-sheeted form deviate from the model at all the loadings. It is clear from the nature of the Mooney plots ($S = 1.35$) up to 40-phr filler loading, that it will steeply increase for further filler loadings. The general nature of the Mooney equation, i.e. a modulus value which tends to infinity at higher filler loadings, which has been reported previously [47,49] is observable here also. It has already been experimentally established by Nielsen [49] that S increases with decreasing particle size. This means that the tendency of finer filler to agglomerate is greater compared to large fillers. Therefore, it is clear that in order to have a reasonable fitting of tensile strengths of the size 1 filler with the Mooney model, different and variable values of S for different loadings, size, etc., must still be suggested. The above observed fitting of theoretical

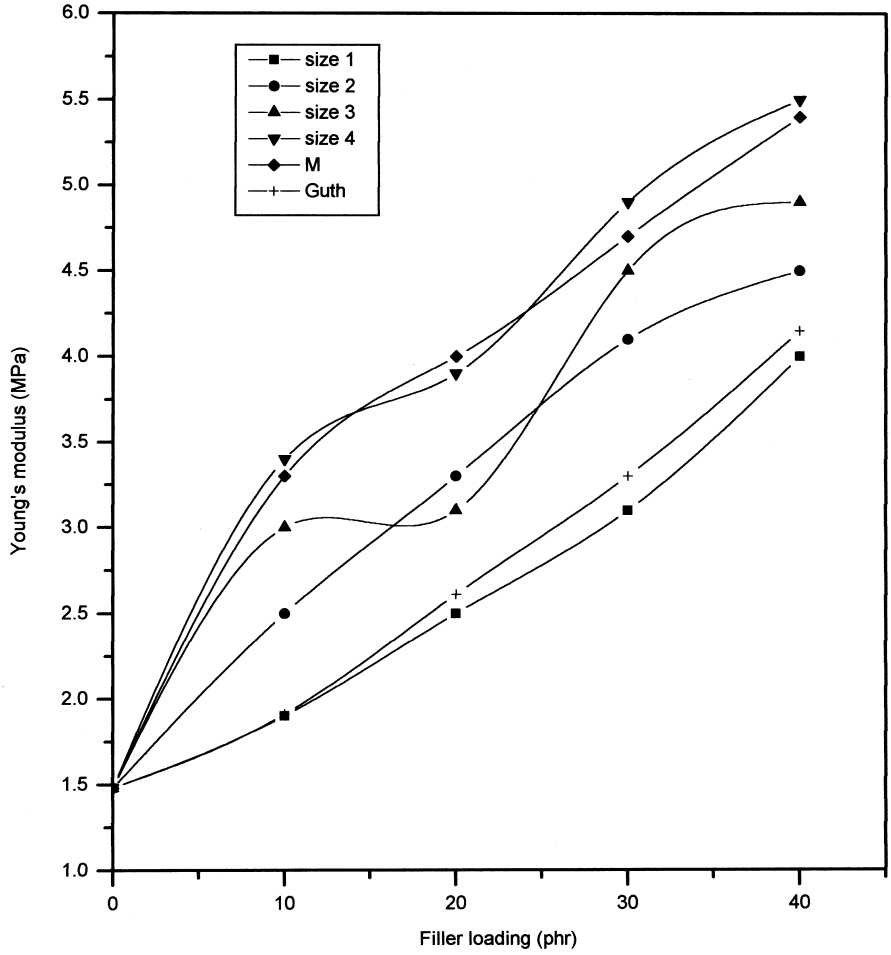

Fig. 17. Comparison of the experimental data with Guth's model for an EV system.

values, even though partial, may be due to the fulfilment of some of the assumptions connected with the Mooney model, such as Poisson's ratio of the matrix must be 0.5, etc. This model also assumes that filler particles are uniformly distributed spheres with good adhesion to the matrix and the modulus of the filler is infinitely greater than that of the matrix. Even when the value of S is 1, the deviations from the model shown by various particle sizes of fillers is almost the same.

Guth and Smallwood [50] generalised Einstein's concept and introduced a particle interaction term. This modified equation can be written as:

$$M_c = M_m(1 + 2.5V_f + 14.1V_f^2) \quad (11)$$

where M_c, M_m and V_f are the same as explained earlier.

For the conventional vulcanisation system, the Guth model gives similar values as given by large-size fillers (size 4) and the mill-sheeted form at 10 and 20 phr. This is clear from Fig. 16. Size 1 and 2 plots, owing to their superior reinforcing behaviour, lie above the model at 30-phr loading. However, at 40-phr filler content, finer fillers sizes 1 and 2 suffer from particle agglomerations and, therefore, their modulus values slightly bend towards the x-axis and lie equidistant from the model. Such a blending is observed for size 4 and the mill-sheeted form also. At higher filler loading, size 3 filler prefers an intermediate position. Since the model does not account for the agglomeration effects at higher loadings, the theoretical curve tends to infinite position, as in the case of the Mooney equation.

When the vulcanisation system changes to efficient mode (Fig. 17), most of the finest filler size (size 1), falls below the value predicted by the model. Agreement between theoretical and experimental values is observable at all the filler loadings. All the filler sizes except sizes 3 and 4, exhibit a constantly increasing deviation from the Guth model with loading. It is a general observation that when the vulcanisation system is conventional, good correlation with the model is shown by large particle-size grades of the filler; and when the vulcanisation system is efficient, the place is taken by the finer fillers.

The model assumes that the change in elastic constant of the rubber by embedded spheres is entirely analogous to the theory of viscosity. For example, when a carbon black suspension undergoes stretching, the suspended particles perturb the stresses and strains are set up in the body,

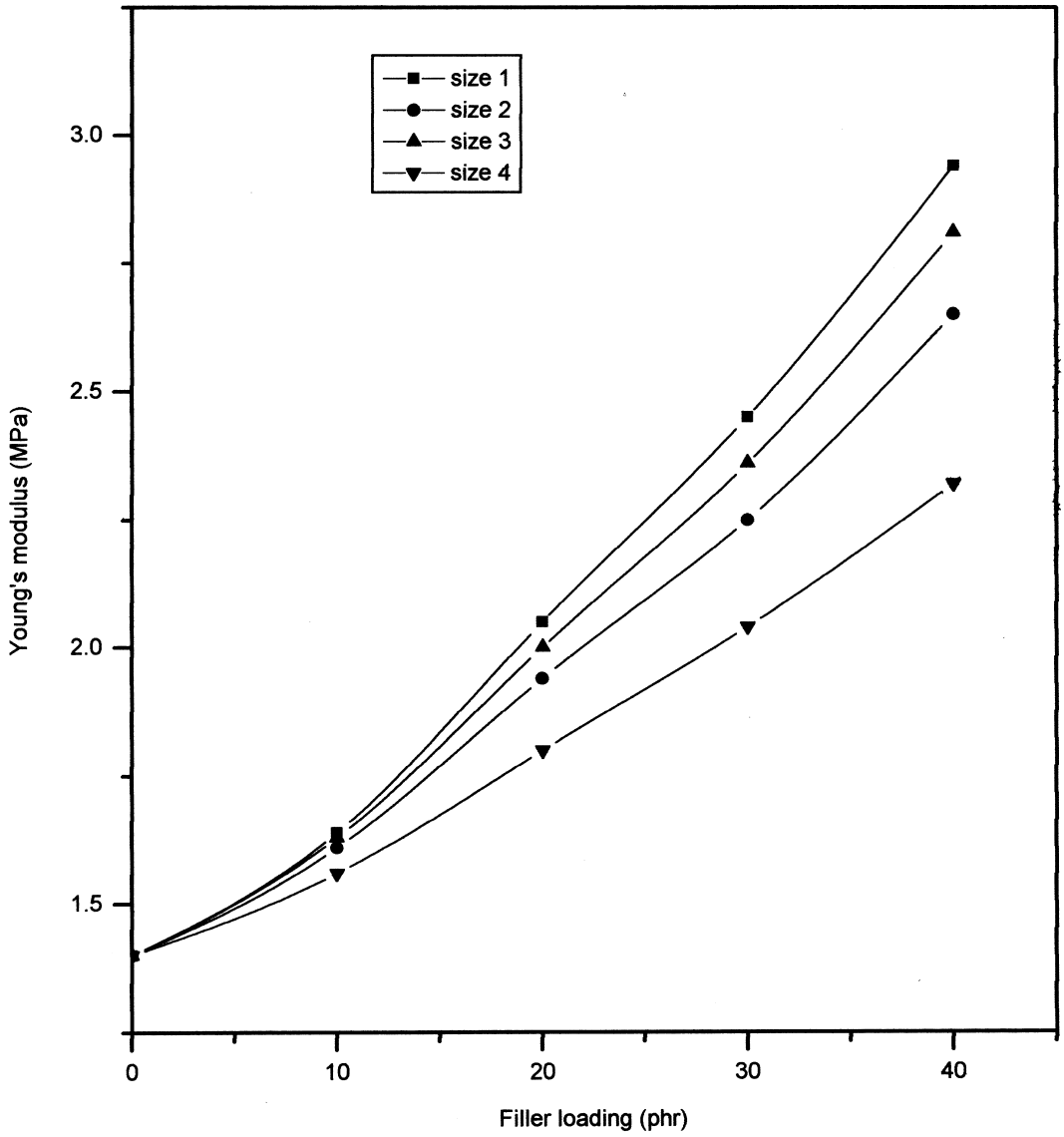

Fig. 18. Theoretical plots of tensile strength from Cohan's model (CV system).

which lead to an increased elastic energy and elastic constants. For this to happen, however, filler particles must be spherical and rigid. Even though sizes 3 and 4 assume a somewhat spherical shape, their non-rigid nature violates the assumption. Therefore, they deviate from the model mainly at higher loadings.

Most of the equations discussed above assume that the particulate inclusion is spherical in shape. Even though we have assumed that filler particles are spherical in the present case, they are not exactly so. Only large particle-size fillers can be considered as spherical, while smaller fillers possess different shapes. This can be understood from a comparison between Figs. 26a (size 1), 29a or 29c (size 4). Many studies have been reported in which the effect of particle shape on reinforcement is discussed. This effect must be treated separately from usual effects such as agglomeration and interphase adhesion.

Properties of composites are affected by changes in the shape of inclusion also. Bueche observes [51] that different filler shapes lead to different mechanical properties. A theoretical treatment was suggested by Wu [52], which could prove that disc-shaped particles can reinforce better than spherical or needle-shaped ones. The anisotropy associated with this, which Wu neglected, was taken into account by Chow [53]. Chow [53] modified the equation by introducing longitudinal and transverse moduli and proved that fillers with a high aspect ratio show a better reinforcement, than those with high particle symmetry. This aspect ratio also is included in the Guth equation modified by Cohan.

The Cohan model [54] is given by the equation:

$$M_c = M_m(1 + 0.675pV_f + 1.62p^2V_f^2) \quad (12)$$

where M_c and M_m are the same as explained earlier and p is

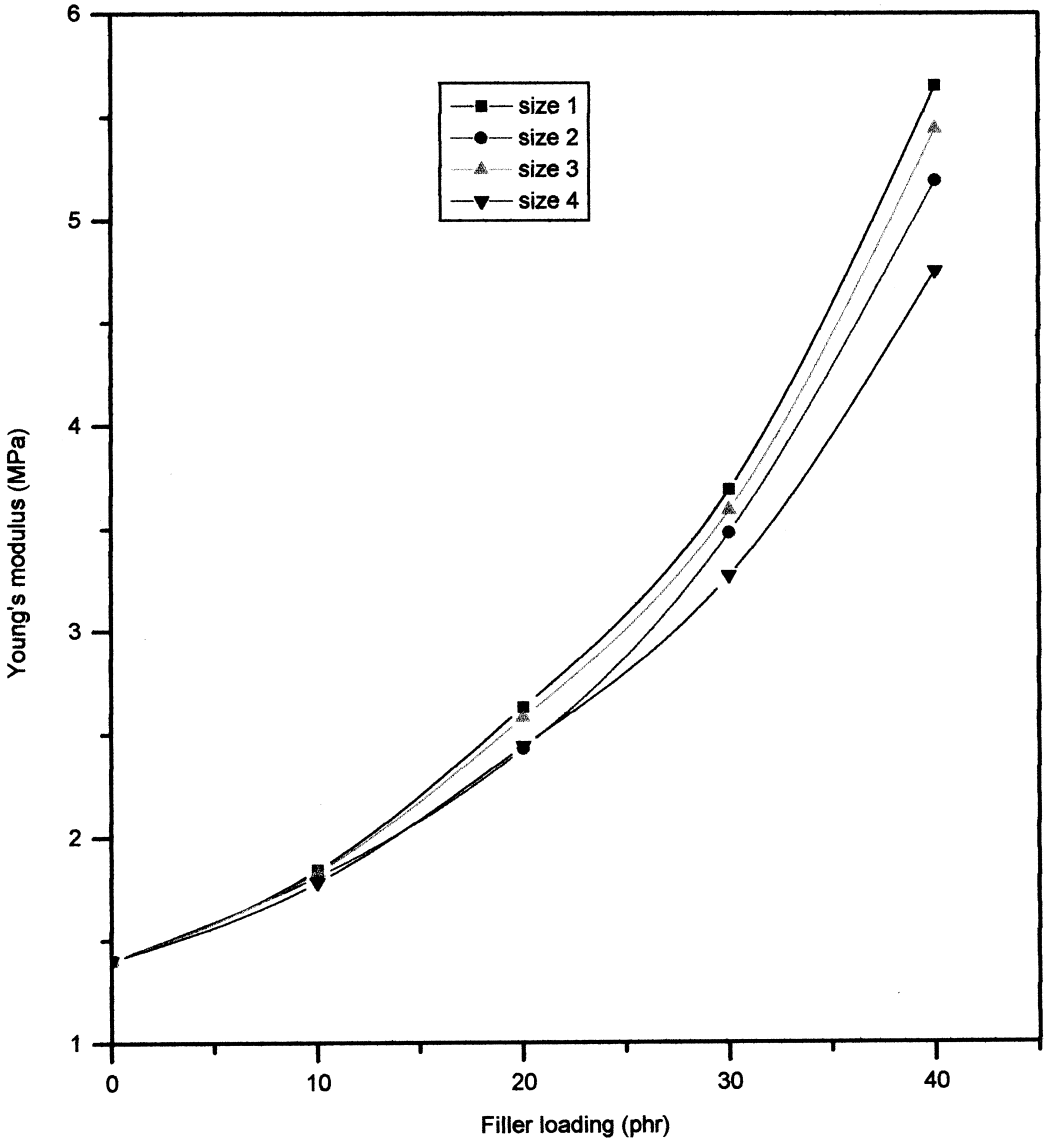

Fig. 19. Theoretical plots of tensile strength from Brodnyan's model (CV system).

the aspect ratio or shape factor, which is the length-to-width ratio of filler particles.

The values of p determined for different particle sizes are given in Table 3. It is clear from Eq. (12) that the modulus of the composite predicted by the equation will be the highest for the case with the maximum value of p. Among the theoretical plots obtained for the different size grades in Fig. 18, size 1 shows the most superior performance. The model is able to predict the order of modulus variation as the particle size decreases. It is assumed by the model that $p \gg 1$, which is not correct as far as our system is concerned. This is clear from the shape factor value given in Table 3. Therefore, deviations from the experimental values can be normally expected.

There is another approach to explain the superior performance of the finest filler in the conventional vulcanisation system. This can more clearly illustrate the expected behaviour when spherical particles are stretched to form rod-shaped particles. Kuhn and Kuhn in the literature [49] derived an expression for the viscosity of suspension of randomly oriented rod-like or cigar-shaped particles in the form of ellipsoids. This equation was modified by Brodnyan [55] for elongated ellipsoids as:

$$M_c = M_m \exp\{2.5V_f + 0.407(p-1)^{1.508}V_f\}/1 - S(V_f) \quad (13)$$

where M_c, M_m, V_f and S are the same as given earlier and p is the aspect ratio ($1 < p < 15$).

The theoretical plots for Young's modulus for the conventional vulcanisation system from the Brodnyan model are presented in Fig. 19. The steeply rising trend of the plots shown by the model compared to the Cohan model (Fig. 18) is observable here. The values of p are the same as

Table 6
Swelling index values

Filler loading (phr)	Gum	Size 1	Size 2	Size 3	Size 4	M
0	408					
10		411	416	422	428	430
20		417	421	427	430	436
30		420	425	429	435	441
40		424	429	436	439	454

already reported (Table 3) and this equation also is found to be successful in predicting the comparatively better reinforcement in the case of finer fillers. Still, deviations from theoretical values can be expected. This is because the model assumes random orientation of rod-shaped fillers, whereas in the present case they are found to be oriented. This orientation results from the shearing in the two-roll mixing mill. This is clear from Fig. 26a. This model predicts that the higher the concentration of rod-like particles, the higher the modulus value. However, it neglects the anisotropy in property associated with their alignment in the matrix. From these discussions it is clear that the models, namely the Cohan and Brodnyan models, can explain the relative order of performance of different size grades in the conventional vulcanisation system only. The trend in the EV system, where larger fillers are more reinforcing, cannot be explained unless these two models are modified appropriately. Moreover, from the theory of all the models described above, the rubber matrix must have the same properties as the unfilled vulcanisate ($V_f = 0$) if a direct experimental test is to be possible. This condition will never be met and, therefore, deviation from different models can be justified. For the present cases, these equations can only be considered as semiquantitative guides for predicting the modulus of composites containing less-rigid soft fillers in a soft matrix.

3.4. Solvent transport studies and cross-link density determination

The swelling index value, which is a measure of the swelling resistance of the rubber compound, is calculated using the equation:

$$\text{Swelling index}\% = A_s/W_1 \times 100 \quad (14)$$

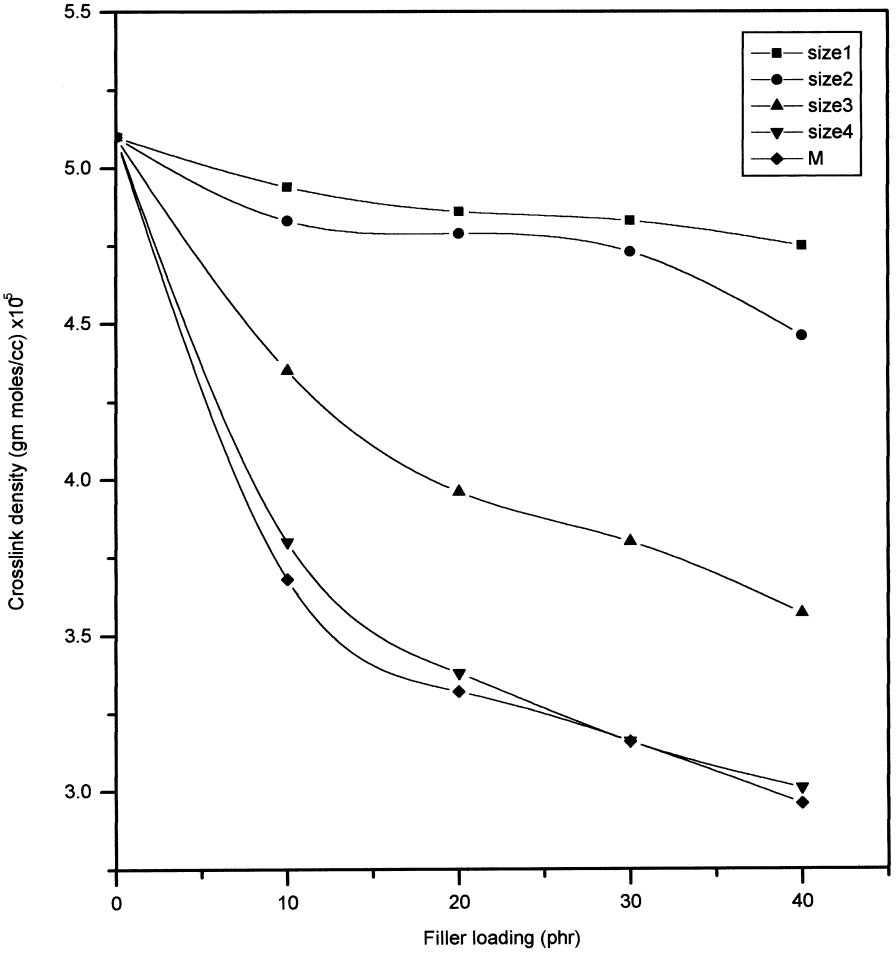

Fig. 20. Effect of filler loading and size on the cross-link density of ENR vulcanisates.

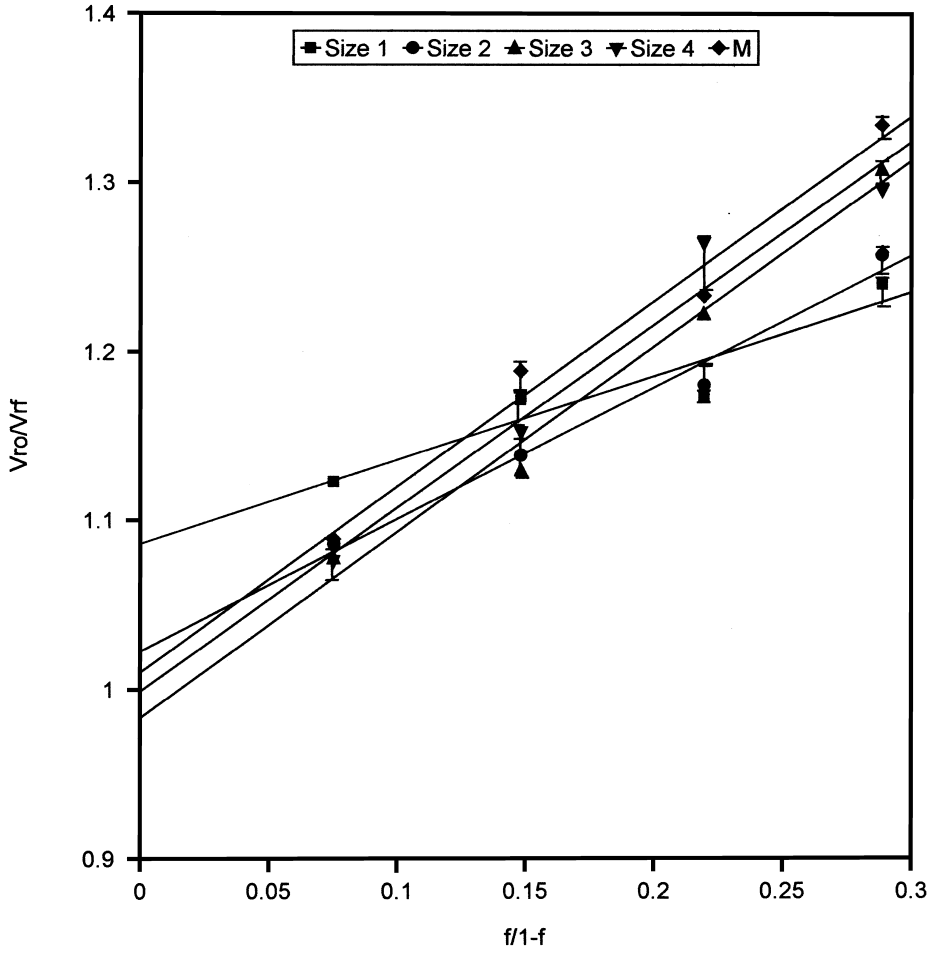

Fig. 21. Variation of V_{ro}/V_{r_f} as a function of filler loading (Kraus plots).

where A_s is the amount of solvent absorbed by the sample and W_1 is the initial weight of the sample before swelling.

It has already been reported in the literature [56,57] that in the case of various polymer solvent systems, differences in the solubility parameter (and hence interaction parameter) values can be used to characterise the sorption behaviour of the solvent. However, our analysis proved that such a correlation is ineffective since the diffusion behaviour of elastomer-filled elastomer systems are more dependent on the compact nature of the sample. This fact is strongly supported by the literature [58]. Since the compact nature of the ENR sample decreases with the addition of prophylactics, the diffusion of the solvent through the sample also increases. It has also been reported in the literature [59] that the diffusion mechanism in rubbery polymers is essentially connected with the ability of the polymer to continually provide opportunities for the solvent to progress in the form of randomly generated voids. Since the ease of void generation in the sample increases with the addition of prophylactics, the uptake of the solvent also increases. Therefore, as the filler content increases, the swelling index value increases for all size grades (Table 6). The solvent absorption by the latex filler particles is found to be minimum for the size 1 filler. This again confirms that in an ENR matrix cross-linked by a CV system, the size 1 filler shows good adhesion. This behaviour is supported by the cross-linked density values (Fig. 20). As the filler content increases, the cross-link density values are found to decrease. This effect can be explained using the basic equations used for swelling:

$$M_C = -\rho_r V_s V_{r_f}^{1/3} / \ln (1 - V_{r_f}) + V_{r_f} + \chi V_{r_f}^2 \quad (15)$$

where M_C is the molecular weight of the polymer between two cross-links ρ_r is the density of the polymer, V_s is the molar volume of solvent and χ is the interaction parameter, which is given by the Hildebrand equations [60,61]:

$$\chi = \beta + \frac{V_s}{RT}(\delta_s - \delta_p)^2 \quad (16)$$

where β is the lattice constant, V_s is the molar volume, R is the universal gas constant, T is the absolute temperature, δ_s is the solubility parameter of the solvent, δ_p is the solubility parameter of the polymer and V_{r_f} is the volume fraction of elastomer in the solvent swollen filled sample and is given

Table 7
Values of slopes and C

Particle size	Kraus equation slope (m)	C	Cunneen and Russell equation slope (a)	Lorenz–Park equation slope (a)
S1	0.4961	0.9946	−0.6790	−1.3979
S2	0.7789	1.2070	−1.0532	−1.5344
S3	1.0979	1.4467	−1.5003	−2.1026
S4	1.0833	1.4357	−1.5067	−2.1725
M	1.0956	1.4449	−1.5107	−2.2144

by the equation by Ellis and Welding [62]

$$V_{r_f} = \frac{(d - fw)\rho_p^{-1}}{(d - fw)\rho_p^{-1} + A_s\rho_s^{-1}} \quad (17)$$

where d is the deswollen weight of the sample, f is the volume fraction of the filler, w is the initial weight of the sample, ρ_p is the density of the polymer, ρ_s is the density of the solvent and A_s is the amount of solvent absorbed by the sample.

As the filler content increases, the amount of solvent absorbed by the sample (A_s) increases, which leads to lowering of V_{r_f} and this in turn reduces the cross-link density values as evident from Fig. 20. It is to be noted that the cross-link density decrease is minimum for finer filler sizes 1 and 2, which have comparatively more reinforcing action in ENR for the CV system and, therefore, they absorb a minimum quantity of solvent. So the cross-link density values (from swelling studies) presented here have good correlation with filler–matrix interface adhesion.

3.5. Extent of reinforcement

The extent of filler reinforcement can be analysed by

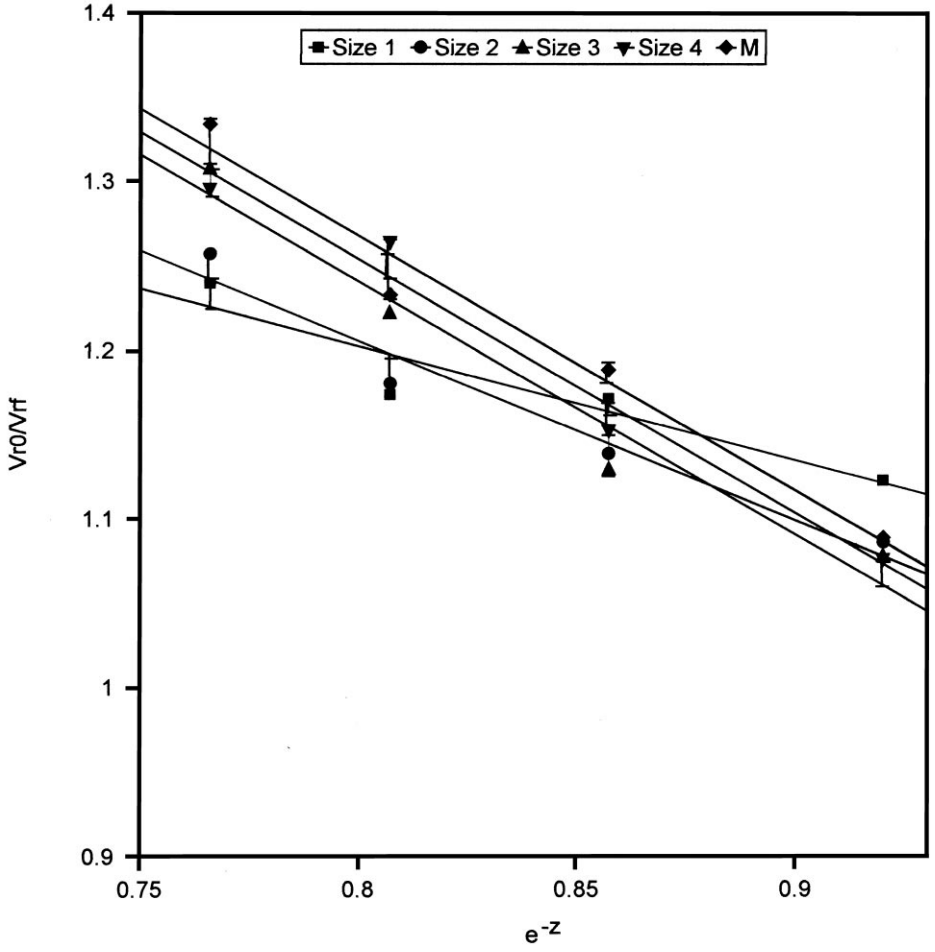

Fig. 22. Variation of V_{ro}/V_{r_f} as a function of filler loading (Cunneen–Russell plots).

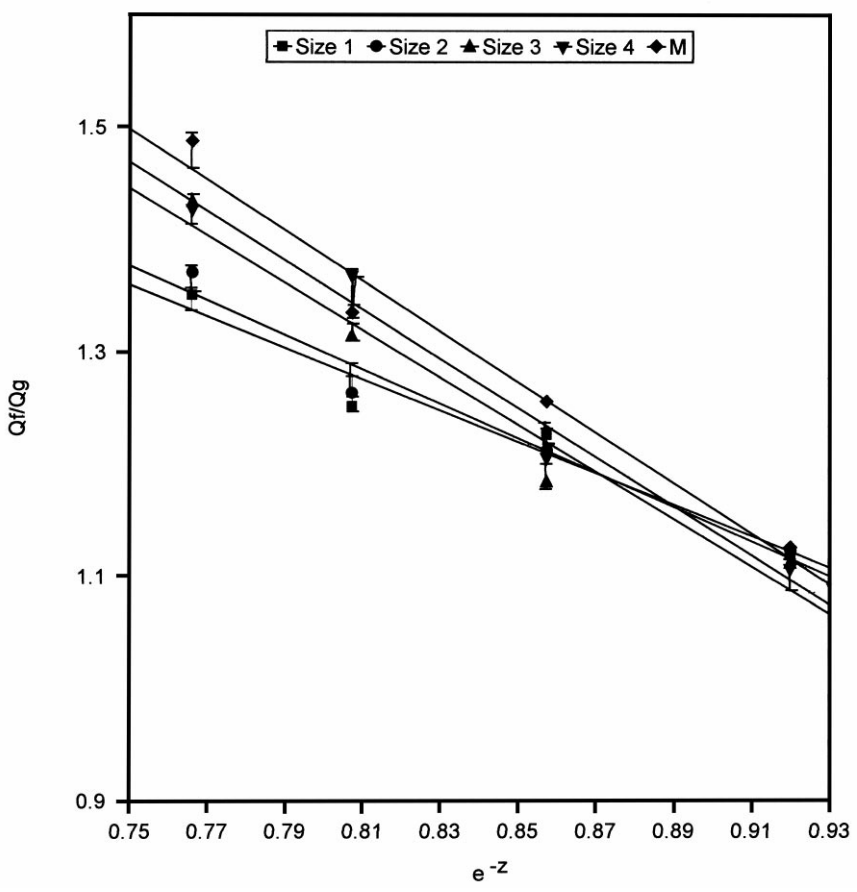

Fig. 23. Variation of Q_f/Q_g as a function of filler loading (Lorenz–Park plots).

using Kraus [35], Cunneen and Russell [36] and Lorenz–Park [37] equations. The Kraus equation is:

$$V_{r_0}/V_{r_f} = 1 - m(f/1 - f) \tag{18}$$

where V_{r_f} is the same as explained above and V_{r_0} is the volume fraction of elastomer in the solvent swollen unfilled sample. Since the above equation is in the form of a straight line, a plot of V_{r_0}/V_{r_f} versus $f/1 - f$ should give a straight line, whose slope (m) will be a direct measure of the reinforcement of the filler. The constant C given by the equation:

$$C = \frac{m - V_{r_0} + 1}{3(1 - V_{r_0}^{1/3})} \tag{19}$$

which is characteristic of the filler, is calculated also. The Kraus plots obtained are given in Fig. 21 and the slope values are presented in Table 7. According to the theory by Kraus, reinforcing fillers such as carbon black will have a negative higher slope. In the present case, we observed that as the filler loading increases, the solvent uptake of the sample also increases. As already explained, this will cause a reduction in V_{r_f} values, which will increase the ratio V_{r_0}/V_{r_f}, since V_{r_0} is constant. This behaviour leads to a positive slope in every case. Since size 1 filler exhibits a minimum positive value of the Kraus slope, it is clear that its solvent absorption is minimum, thereby supporting its better adhesion with the ENR matrix in the CV system. Moreover, constant C is inversely related to filler agglomeration tendency. It is also clear from Table 7 that the finest filler size 1 has maximum tendency for agglomeration. The trend given by the C value in the Kraus equation is in agreement with S, the crowding factor given by Mooney [47]. It has also been experimentally proved [47] that the S value increases with reduction in particle sizes. This means an increase in the ratio of apparent volume occupied by the filler to true volume, which points to the case of filler agglomerations. Thus, the higher tendency of the size 1 filler for agglomeration can be justified.

The Cunneen–Russell equation is

$$V_{r_0}/V_{r_f} = a\, e^{-z} + b \tag{20}$$

where V_{r_0} and V_{r_f} are the same as explained earlier, z is the weight fraction of the filler, a and b are constants. Here a plot of V_{r_0}/V_{r_f} versus e^{-z} should give a straight line with negative slope (a). V_{r_0}/V_{r_f} is found to increase with increasing filler loading as clear from Fig. 22. This increase is extensive in the case of large-size fillers (size 4 and M). For finer fillers, sizes 1 and 2, which are comparatively highly reinforcing, the absorption of the solvent is minimum,

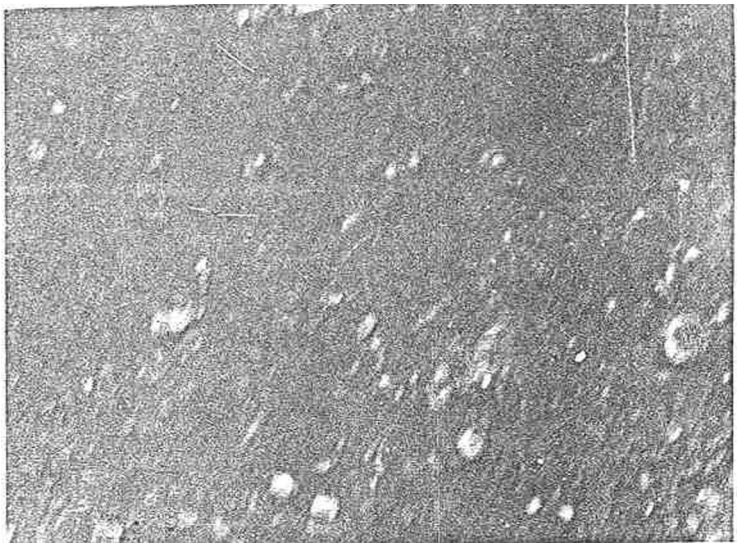

Fig. 24. SEM fractograph of tensile gum specimen.

which results in a lower V_{r_0}/V_{r_f} ratio and a smaller negative slope.

The Lorenz–Park equation is

$$Q_f/Q_g = a\,e^{-z} + b \tag{21}$$

where Q is defined as the amount of solvent absorbed/gm of rubber and is given by

$$Q = \frac{\text{Swollen weight} - \text{dried weight}}{\text{Original weight} \times 100/\text{formula weight}} \tag{22}$$

The subscripts f and g refer to filled and gum vulcanisates, respectively. z is the weight fraction of the filler. A plot of Q_f/Q_g versus e^{-z} gives a straight line with negative slope (Fig. 23). As explained earlier, here also finer fillers (sizes 1 and 2) exhibit lower slope, proving their better adhesion with ENR.

All the above previously established equations support the superior performance of the size 1 filler compared to large-size fillers when a CV system is used for the cross-linking of ENR.

3.6. Fractographic analysis

The improvement in tensile and tear performance with loading of filler is supported by the morphology of the fractured surfaces. These fractographs are presented in Figs. 24–30. Since the presence of filler particles is clearly visible in all the filled cases, this latex-filled ENR system can be considered only as a composite material. All the composite samples exhibit a two-phase morphology.

The fractograph of the gum vulcanisate is presented in Fig. 24. The smooth fractured surface observed here is

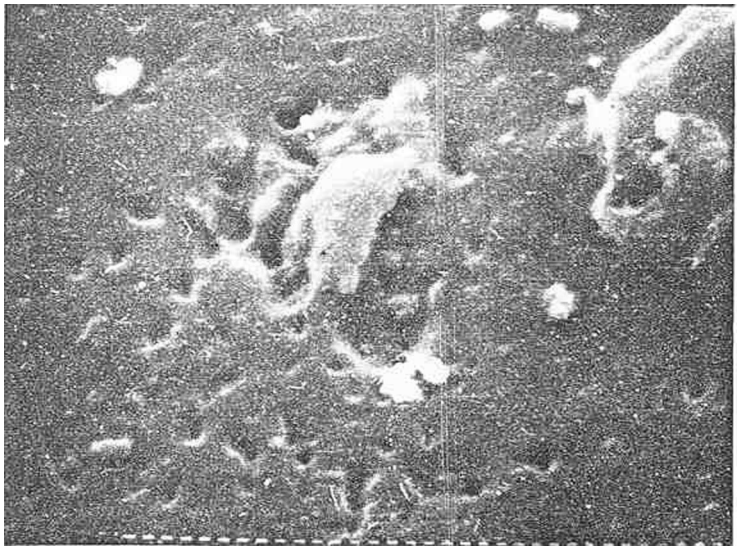

Fig. 25. SEM fractograph of tear gum specimen.

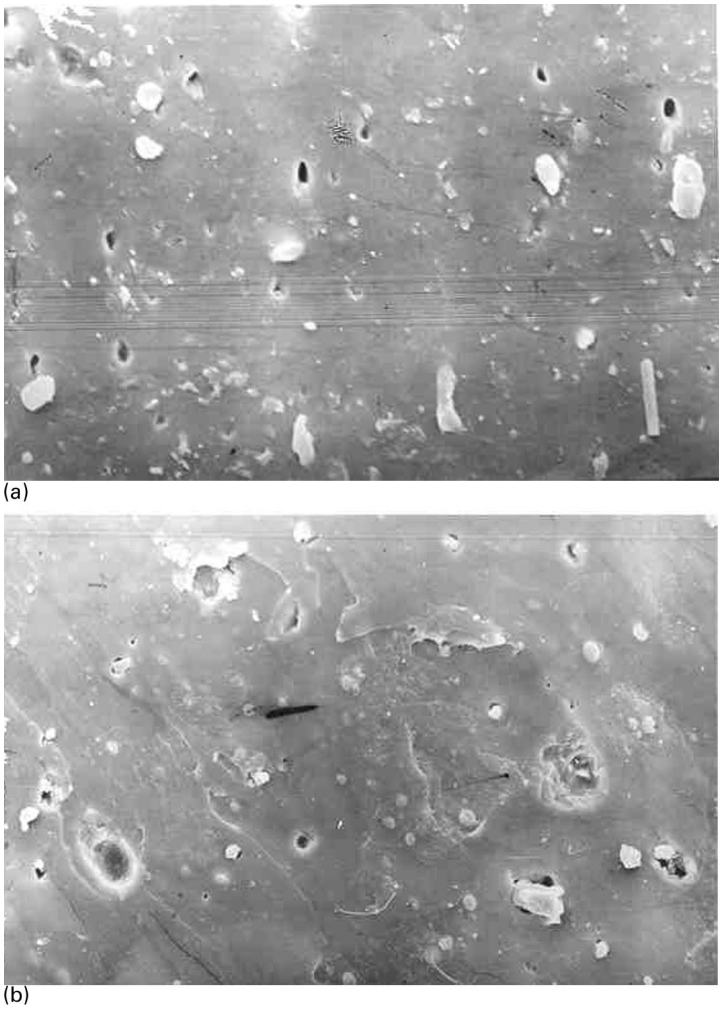

Fig. 26. (a,b) SEM fractograph of tensile specimen filled with 10 phr of size 1 filler.

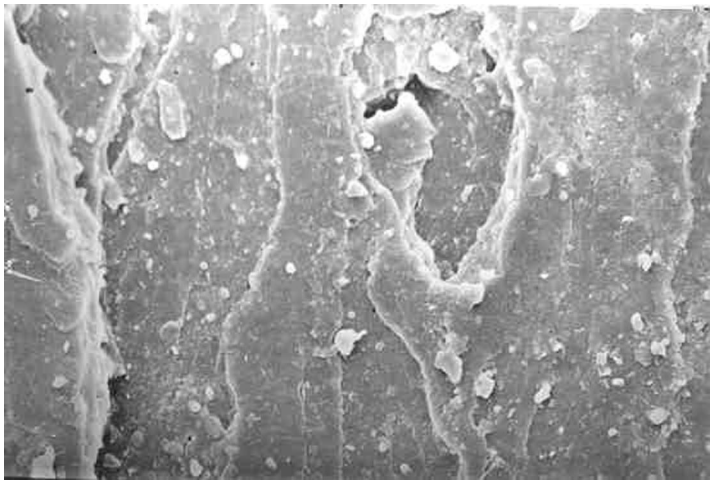

Fig. 27. SEM fractograph of tensile specimen filled with 30 phr of size 1 filler.

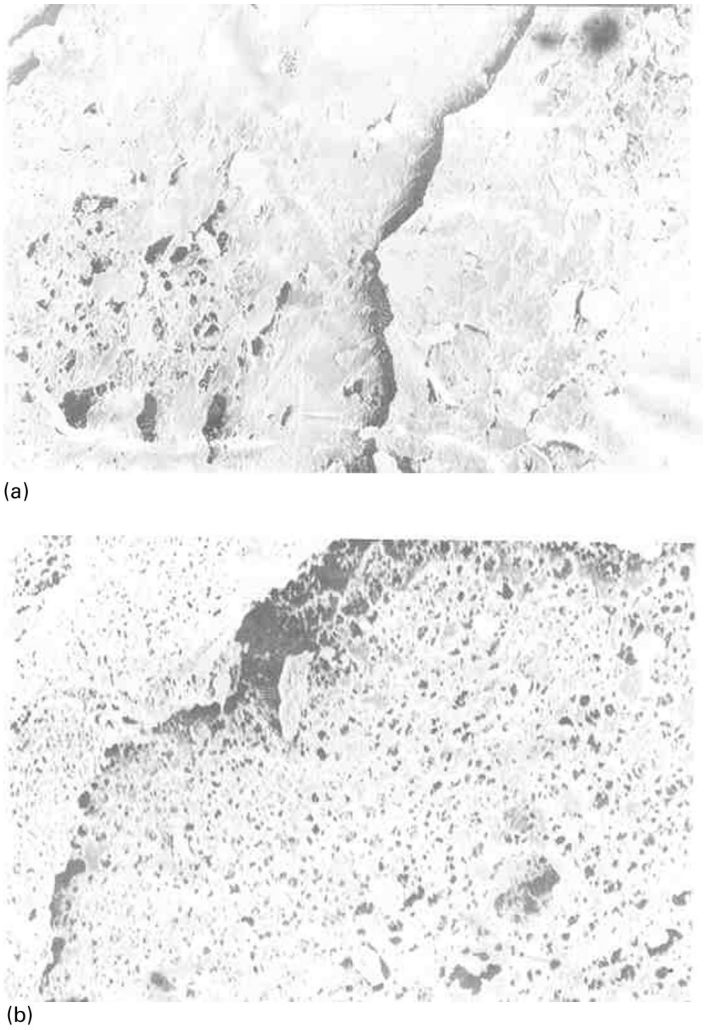

Fig. 28. (a,b) SEM fractograph of tear specimen filled with 40 phr of size 1 filler.

characteristic of low-strength vulcanised materials. In the case of torn surfaces of gum vulcanisates also, a similar morphology could be observed. The weak mechanical strength of the gum is clear from the undeviated cracks in Fig. 25.

In the case of ENR filled with 10 phr of size 1 filler, the fractography reveals the presence of fine filler particles (Fig. 26a). The presence of cigar-shaped particles aligned in a particular direction also is observable. Moreover, the fracture is found to deviate only slightly (Fig. 26b) presenting incomplete parabolic patterns. This confirms the comparatively high strength of the material. Still, dewetting is present in Fig. 26a. Fig. 27 is the tensile fractured surface of the ENR sample filled with 30 phr of size 1 filler. Here the cracks are extensive and much deviated. Such parabolic fractured surfaces support the high strength of the material. The role of filler particles in blocking the advancing crack also is observable. The torn surface of ENR filled with 40-phr size 1 filler is presented in Fig. 28a and b. Here also crack deviation is extensive. The portions from which the filler particles are debonded are visible as holes in the figure. The filler particles elongate to high strains and obstruct the tear (Fig. 28b). Thus, as explained above, the material filled with size 1 filler shows superior tear performance.

For fillers of higher sizes (size 4) at a loading of 10 phr, debonding is extensive. Also the cracks are again becoming smooth. Dewetting is clear from Fig. 29a and b and smooth fractures are visible in Fig. 29b and c. It can be seen from Fig. 29c that the particle size of fillers is not uniform. This is because large-size fillers undergo more size reduction during mixing.

Fig. 30 is the torn surface of ENR filled with 30-phr size 4 filler. The material shows cracks with slight deviations, which proves its good tear strength. The accumulation of filler particles on the crack path in an effort to prevent the advancing crack is visible in the figure. It is a general observation in Figs. 29c and 30 that the larger-size grade (size 4) filler particles are polydispersed in size owing to their breakage during mixing.

For most of the filled cases, the fractured surfaces are

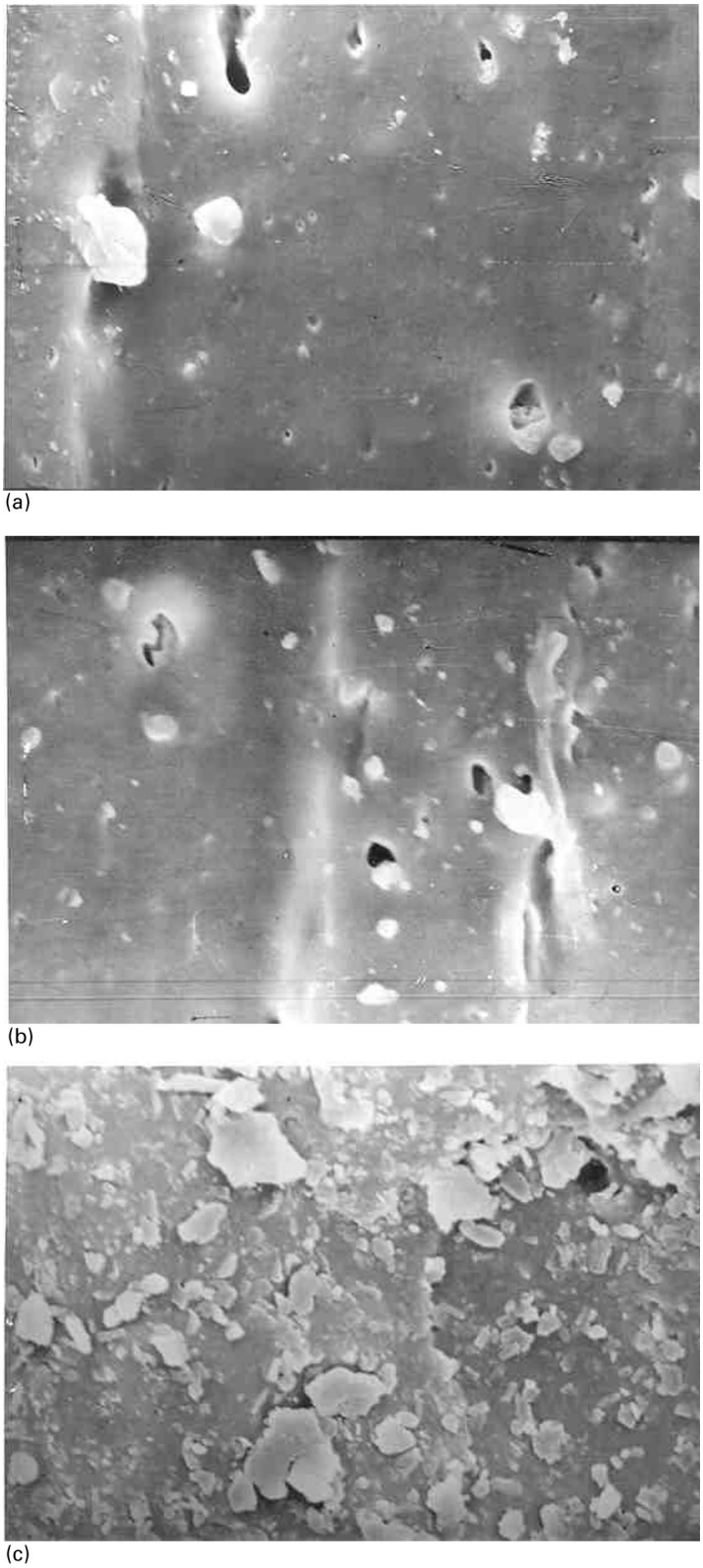

Fig. 29. (a–c) SEM fractograph of tensile specimen filled with 10 phr of size 4 filler.

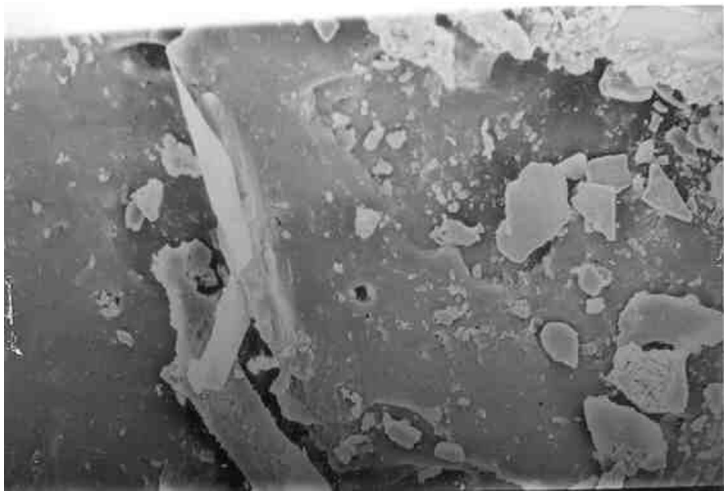

Fig. 30. SEM fractograph of tear specimen filled with 30 phr of size 4 filler.

greatly crack deviated and present a series of parabolic lines distributed all over the surfaces. Such behaviour is due to the interaction of main fracture fronts with subsidiary fracture fronts and from the resistance in tear propagation by filler particles. Thus the superior mechanical performance of size 1 filler is strongly supported by the SEM fractographic studies.

4. Conclusions

The utilisation of cross-linked waste natural rubber as a potential filler in ENR deserves much attention. The cross-linked waste rubber has been powdered and sieved into different particle sizes. The morphology and size distribution of these particles has been analysed. It has been observed that, as the filler content increases, the curing characteristics like optimum cure time, scorch time and induction time decrease. The cure-activating nature of the filler is clear from the increase in cure rate index and rate constant values. The filler helps the compounder by reducing the sticky nature of epoxidised natural rubber compound during mixing. These observations are advantageous as far as processability and productivity are concerned. In the case of the conventional vulcanisation system, where sulphur migration is absent, finer filler shows superior tensile performance than size 4 and the mill-sheeted form of the filler. However, in efficient vulcanisation systems, where sulphur migration plays a role, the order of performance is inverted. The theoretical models such as those of Einstein, Mooney, Guth, Cohan, and Brodnyan are found to deviate from the experimental observations. Still the experimentally observed order of performance for different size grades of the filler could be correctly depicted by the Cohan and Brodnyan models. The three-layer model used here has been found to be completely successful in understanding the phenomena of sulphur migration in the efficient vulcanisation system and its extent in the case of different particle sizes of the fillers. As far as tear strength is concerned, size 1 filler has proved to be the best, but in every case, the property drops at 40-phr loading. The swelling index values register a constant increase with loading of filler and this increase is minimum for fine fillers such as size 1. In addition to this, the reduction in cross-link density with filler loading also is minimum for size 1 filler. The comparatively better adhesion between epoxidised natural rubber and size 1 filler is proved by previously established equations like the Kraus, Cunneen and Russell and Lorenz–Park equations. The scanning electron micrographs of fractured surfaces clearly support the good particle–matrix adhesion in the case of fine fillers. The non-compatible and phase-separated nature of the filler particles in the epoxidised natural rubber matrix cause these materials to be classified only as a filled epoxidised natural rubber composite, rather than as a blend system.

Acknowledgements

One of the authors (G.M.) is thankful to the Council of Scientific and Industrial Research, New Delhi, for the financial support.

References

[1] Debnath S, De SK, Khastgir D. J Appl Polym Sci 1989;37:1449.
[2] Debnath S, De SK, Khastgir D. J Mater Sci 1987;22:4453.
[3] Swor RA, Jensen LW, Budzol M. Rubber Chem Technol 1980;53:1215.
[4] Phadke AA, Bhattacharya AK, Chakraborthy SK, De SK. Rubber Chem Technol 1983;56:726.
[5] Rajalingam P, Sharpe J, Baker WE. Rubber Chem Technol 1993;66:664.
[6] Acetta A, Vergnaud JM. Rubber Chem Technol 1981;54:302.
[7] Drozdovskii VF. Int Polym Sci Technol 1992;19(11):T/57.
[8] Phadke AA, Chakraborthy SK, De SK. Rubber Chem Technol 1984;57:19.
[9] Phadke AA, Kuriakose B. Kautsch Gummi Kunstst 1985;38:694.

[10] Claramma NM, Thomas KT, Thomas EV. Paper presented at the Rubber Conference, Jamshedpur, 6–8 November 1986.
[11] Aziz Y. Paper presented at Polymer 90, Kuala Lumpur, Malaysia, 23 September 1990.
[12] Pittolo M, Burford RP. Rubber Chem Technol 1985;58:97.
[13] Air products Ltd, Appln 2, 022, 105, 12 December 1979.
[14] Duhaime JRM, Baker WE. Plast Rubber Compos Process Appl 1991;15(2):87.
[15] Oliphant K, Baker WE. Polym Engng Sci 1993;33(3):166.
[16] Tukachinsky A, Schworm D, Isayev AI. Rubber Chem Technol 1996;69:92.
[17] Levin VYu, Kim SH, Isayev AI, Massey J, Meerwall Evon. Rubber Chem Technol 1996;69:104.
[18] Isayev AI, Chen J, Tukachinsky A. Rubber Chem Technol 1995;68:267.
[19] Isayev AI, Yushanov SP, Chen J. J Appl Polym Sci 1996;59:803.
[20] Fujimoto K. Nippon Gomu Kyokaishi 1979;52:281.
[21] Creasey JR, Wager MP. Rubber Age 1968;100(10):72.
[22] Fujimoto K, Nishi T, Okamoto T. Int Polym Sci Technol 1981;8(8):T/30.
[23] Fujimoto K, Nishi T, Okamoto T. Int Polym Sci Technol 1981;8(8):T/65.
[24] Yasuda H, Marsh C, Brandt S, Reilly CN. J Polym Sci Polym Chem 1977;15:991.
[25] Zimmerman CJ, Ryde N, Kally N, Partch RE, Matijevie E. J Mater Res 1991;6:855.
[26] Blythe AR, Briggs D, Kendall CR, Rance DG, Zichy VJI. Polymer 1978;19:1273.
[27] Eaves JM. J Adhes 1973;5:1.
[28] Singh A. Potential modification of polyblends by irradiations. In: International Conference on Advances in Additives, Modifiers and Polymer Blends, Miami, Florida, 1992.
[29] Yu DW, Xanthos M, Gogos CG. Polym Mater Sci Engng 1992;67:313.
[30] Nasir M, Choo CH. Eur Polym J 1989;25(4):355.
[31] Baker CSL, Gelling IR, Newell R. Rubber Chem Technol 1994;58:67.
[32] Davis CKL, Wolfe SV, Gelling IR, Thomas AG. Strain crystallization on random copolymer produced by epoxidation of *cis*-1,4-polyisoprene. Polymer 1983;24:107.
[33] Grebenkina ZI, Zakharov ND, Volkova EG. Int Polym Sci Technol 1978;5(11):2.
[34] Gorton ADT, Pendle TD. NR Technol 1976;7(4):77.
[35] Kraus G. J Appl Polym Sci 1963;7:861.
[36] Cunneen JI, Russell RM. Rubber Chem Technol 1970;43:1215.
[37] Lorenz O, Parks CR. Rubber Chem Technol 1961;50:299.
[38] Sharapova LN, Chekanova AA, Zakharov ND, Borisova EYu. Int Polym Sci Technol 1983;10:4.
[39] Furtado CRG, Nunes RCR, De AS Siqueira Filho. Eur Polym J 1994;30(10):1151.
[40] Lewis, Nielsen LE. J Appl Polym Sci 1970;14:1449.
[41] Ahmed S, Jones FR. Composites 1988;19:277.
[42] Spanoudakis J, Young R. J Mater Sci 1984;19:487.
[43] Einstein A. Investigation on theory of Brownian motion. New York: Dover, 1956 (English translation).
[44] Edwards DC. J Mater Sci 1990;25:4175.
[45] Mathew G, Singh RP, Lakshminarayanan R, Thomas S. J Appl Polym Sci 1996;61:2035.
[46] Phadke AA, Bhowmick AK, De SK. Rubber Chem Technol 1985;58:4063.
[47] Mooney M. J Colloid Sci 1951;6:162.
[48] Payne AR. In: Krause G, editor. Reinforcement of elastomers. New York: Wiley-Interscience, 1965. p. 76.
[49] Nielson LE. J Comput Mater 1967;1:100.
[50] Guth E. J Appl Phys 1951;16:21.
[51] Bueche AM. J Polym Sci 1957;25:139.
[52] Wu TT. Int J Solids Struct 1966;2:1.
[53] Chow TS. J Polym Sci Polym Phys Ed 1978;16:959.
[54] Cohan LH. India Rubber World 1947;117:343.
[55] Brodnyan JG. Trans Soc Rheol 1959;3:61.
[56] Uragami T, Morikawa T, Okuno H. Polymer 1989;30:1117.
[57] Okuno H, Nishimoto H, Miyata T, Uragami T. Makromol Chem 1993;194:927.
[58] Rhim JIW, Yoon S, Kim SW, Lee KH. J Appl Polym Sci 1997;63:521.
[59] Amerongen GJV. Rubber Chem Technol 1964;37:1065.
[60] Hildebrand JH, Scott RL. The solubility of non-electrolyte. 3rd ed. New York: Van Nostrand Reinhold, 1950 (Dover, New York, 1964).
[61] Hildebrand JH, Scott RL. Regular solutions. Englewood Cliffs, NJ: Prentice-Hall, 1962.
[62] Ellis B, Welding GN. Techniques of polymer science. London: Society for Chemical Industry, 1964 (p. 46).